

On Integrable Nets in General and Concordant Chebyshev Nets in Particular

Michal MARVAN

Mathematical Institute in Opava, Silesian University in Opava,
Na Rybníčku 1, 746 01 Opava, Czech Republic
E-mail: michal.marvan@math.slu.cz

Received March 20, 2024, in final form March 31, 2025; Published online April 28, 2025

<https://doi.org/10.3842/SIGMA.2025.029>

Abstract. We consider general integrable curve nets in Euclidean space as a particular integrable geometry invariant with respect to rigid motions and net-preserving reparameterisations. For the purpose of their description, we first give an overview of the most important second-order invariants and relations among them. As a particular integrable example, we reinterpret the result of I.S. Krasil'shchik and M. Marvan (see Section 2, Case 2 in [*Acta Appl. Math.* **56** (1999), 217–230]) as a curve net satisfying an \mathbb{R} -linear relation between the Schief curvature of the net and the Gauss curvature of the supporting surface. In the special case when the curvatures are proportional (concordant nets), we find a correspondence to pairs of pseudospherical surfaces of equal negative constant Gaussian curvatures. Conversely, we also show that two generic pseudospherical surfaces of equal negative constant Gaussian curvatures induce a concordant Chebyshev net. The construction generalises the well-known correspondence between pairs of curves and translation surfaces.

Key words: integrable surface; integrable curve net; differential invariant; pseudospherical surface; Chebyshev net; concordant net

2020 Mathematics Subject Classification: 37K10; 53A05; 53A55; 53A60

1 Introduction

Classical integrable geometry includes integrable classes of surfaces in Euclidean space as the most familiar instance [11, 39, 69, 84]. Integrability is mostly understood in the sense of soliton theory. Numerous examples are known, often originating in the nineteenth century. A handful have been characterised in terms of differential invariants of surfaces. In particular, Bianchi [8, Section 99] characterised the isometry classes of surfaces of revolution (which correspond one-to-one to planar curves). Well-known are also surfaces satisfying $\Delta(1/H) = 0$, Bianchi surfaces, and some others [11, 39]. A number of known integrable geometries have been characterised in terms of curve invariants. These include, for instance, the Hasimoto surfaces swept by curves moving according to geometrically determined dynamics [40, 69] or the Razzaboni surfaces formed by nets of Bertrand curves [77].

However, quite rare have been successful classification attempts. Those known to the author are limited to integrable Weingarten surfaces and their evolutes, see [5] and references therein, which revealed nothing unrelated to nineteenth-century geometry.

We consider integrable nets as integrable geometries characterisable in terms of net invariants. The paper has grown out of our earlier result [48, Section 2] on integrable Gauss–Mainardi–Codazzi systems under Chebyshev parameterisation. Two main unsolved problems were:

- (A) finding the geometric meaning of the result and
- (B) constructing explicit solutions.

Sections 2 to 6 and Appendix A pertain to problem (A) and Sections 6 to 10 to problem (B).

Section 2 briefly reviews nets, emphasising their description as direction pairs. Section 3 reviews second-order differential invariants, including the Schief curvature [78, Section 3.1]. Section 4 reviews general Chebyshev nets and characterises them in terms of two scalar invariants. Section 5 introduces integrable classes of nets in analogy with integrable classes of surfaces and explains their main differences. Relations among invariants are relegated to Appendix A. In Section 6, we turn to integrable Chebyshev parameterisations found in [48, Section 2] and easily recognise them as classes of nets, which answers problem (A).

The first part may seem unnecessarily extensive, compared to the simple answer it eventually gives to problem (A). However, this part has also the concurrent goal of compensating for the lack of suitable survey literature on nets and their invariants, opening the way to more classification results related to integrable geometries, and possibly also to a new interpretation of old results in planned follow-ups to this article.

As for problem (B), paper [48] only provided a zero-curvature representation (ZCR), which is a standard starting point for obtaining exact solutions [29, 63]. However, we have not been able to turn the ZCR into solutions.

In this paper, we manage to solve problem (B) in the case of *concordant* Chebyshev nets, characterised by the proportionality of the Gauss and Schief curvatures. For this class, vector conservation laws are obtained in Section 7. With their help, we establish a correspondence between concordant Chebyshev nets and pairs of pseudospherical surfaces of equal curvatures, providing a geometric solution to problem (B). The passage from concordant nets to pairs of pseudospherical surfaces is covered in Section 8, the opposite direction in Section 9. The construction generalises the well-known correspondence between translation surfaces and pairs of curves [31, 33, 43, 53] and provides a more or less straightforward way to obtain examples of exact concordant Chebyshev nets, see Section 10.

For simplicity, our exposition is local; smoothness is assumed everywhere.

2 Nets

We consider nets immersed in the Euclidean space \mathbf{E}^3 . They are a classical object of interest in differential geometry [8, 9, 23, 24, 25] and have numerous applications, especially in construction and architecture [49, 64, 68, 85]. Examples include the asymptotic, characteristic, Chebyshev, circular, cone-, conformal, conjugate, equal path, equiareal, geodesic, Hasimoto, LGT, Liouville, orthogonal, principal, Razzaboni, Voss–Guichard, wobbly nets, and plenty of others (e.g., [23, 28, 30, 34, 38, 44, 45, 46, 55, 64, 69, 72, 73, 88, 91] and references therein). Nets also appear as substructures of richer structures such as n -webs, see [1] and references therein. Still other nets appear as smooth limits of discrete nets, which are obligatory substructures of discrete surfaces [12, 13, 14].

By a *local parameterisation* or simply a *parameterisation* of a surface $S \subset \mathbf{E}^3$ we mean a diffeomorphism $\mathbf{r}: U \rightarrow V$, where $U \subseteq \mathbb{R}^2$ is an open subset of the *parameter space* \mathbb{R}^2 and $\mathbf{r}U = V \subseteq S$ is an open subset of the surface S . In this paper, \mathbf{r} and S are always related in this way.

Viewed as maps $\mathbf{r}: U \rightarrow \mathbb{R}^3$, parameterisations can be added and multiplied by functions $U \rightarrow \mathbb{R}$. Thus, parameterisations $\mathbf{r}: U \rightarrow \mathbb{R}^3$ form a $C^\infty U$ -module.

A net on a surface S can be introduced in various equivalent ways, in particular as a pair of transversal foliations of S by curves or as a pair of transversal direction fields on S . Both exist in oriented and non-oriented versions.

Definition 2.1. A *foliation* of an open set $V \subseteq S$ is the partition of V into the level sets $f = \text{const}$ of a function $f: V \rightarrow \mathbb{R}$, $df \neq 0$. Foliations $f_1 = \text{const}$ and $f_2 = \text{const}$ are *transversal* if $df_1 \wedge df_2 \neq 0$. Locally, a *net* on a surface S is a transversal pair of foliations. If $df_1 \wedge df_2 = 0$ at isolated points or lines, these are referred to as *singular*.

The surface S is said to be *supported* by the net.

Definition 2.2. In the notation of Definition 2.1, let \mathbf{r} be a parameterisation of S . Then functions $x_1 = f_1 \circ \mathbf{r}$, $x_2 = f_2 \circ \mathbf{r}$ are called the *family parameters*, with respect to which the curves $f_i = \text{const}$ are the *isoparametric* curves. The net is denoted by $\mathbf{r}(x_1, x_2)$ and said to be *isoparametric*.

Every net on a surface S is locally isoparametric if we choose x_1, x_2 from Definition 2.2 as the local parameters.

Obviously, regular local reparameterisations

$$x'_1 = x'_1(x_1), \quad x'_2 = x'_2(x_2) \quad (2.1)$$

preserve the curve families. Locally, nets can be identified with the equivalence classes of parameterisations modulo reparameterisations (2.1).¹

Differential invariants of curve nets can depend on the orientation. *Oriented nets* can be introduced as the equivalence classes of parameterisations modulo reparameterisations (2.1) satisfying $dx'_i/dx_i > 0$.

Working with parameterisations is not entirely convenient when dealing with several different nets on a surface simultaneously. This can be remedied by employing direction pairs, oriented or non-oriented. For counterparts used in computer graphics see [89, Section 2].

Definition 2.3. A *direction field* $[X]$ represented by a nowhere vanishing vector field X on an open set $V \subseteq S$ is defined by

$$[X] = \{fX \mid f \in C^\infty S, f \leq 0\}.$$

In the oriented version,

$$[X] = \{fX \mid f \in C^\infty S, f > 0\}.$$

A *direction pair* is an ordered pair $([X_1], [X_2])$ of two distinct direction fields.

The fields can be specified in the parameter domain $U \subseteq \mathbb{R}^2$ and mapped to S by the tangent mapping $\mathbf{r}_*: TU \rightarrow TS$, which is tacitly understood in this paper.

Needless to say, nets and direction pairs mutually correspond. In the non-oriented setting, tangent vector fields to curves of a net represent a direction pair, while the trajectories of the generating vector fields form a net. Let us, however, remark that a direction pair can exist globally even if the corresponding net of trajectories does not (recall the irrational flow on a torus).

Obviously, transformations

$$X'_i = f_i X_i, \quad (2.2)$$

where $f_i \in C^\infty S$, $f_i \leq 0$, preserve non-oriented direction fields. Oriented direction fields are preserved if functions f_i are positive.

Transformations (2.1) and (2.2) mutually correspond. In the non-oriented setting, a direction field $[X]$ in \mathbb{R}^2 corresponds to a vector field X modulo the equivalence $X \equiv fX$, $f \leq 0$, which corresponds to a linear homogeneous first-order PDE, which has a general solution of the form $F(x)$, where $Xx = 0$ and $dF \neq 0$. In the oriented setting, the gradients $\text{grad } f_i$ are naturally oriented and have to correspond to the orientations of X_i and of the surface S , which must be orientable.

¹In the literature, transformations (2.1) are sometimes called *Sannian transformations* [28, 71].

Remark 2.4. Weise [93, Section 1] approached nets as isotropic directions of a conformal class of Lorentzian metrics, which became a common approach in the former Soviet literature [42, 66, 82]. This approach provides a connection to binary differential equations [17], but does not distinguish between pairs $([X_1], [X_2])$ and $([X_2], [X_1])$, which prohibits asymmetrically defined nets.

Definition 2.5. Vector fields X_1, X_2 are said to be the *commuting representatives* of a direction pair $([X_1], [X_2])$ if they commute.

Proposition 2.6. *Every direction pair locally possesses commuting representatives.*

Proof. These can be obtained as the vector fields $\partial/\partial x_1$ and $\partial/\partial x_2$ for the family parameters x_1, x_2 (see Definition 2.2) of the corresponding net. ■

Definition 2.7. Denoting by I the metric of S , $I(X, Y) = X\mathbf{r} \cdot Y\mathbf{r}$, the *unit representative* \widehat{X} of a direction field $[X]$ is defined by

$$\widehat{X} = \frac{X}{\sqrt{I(X, X)}},$$

choosing the positive square root.

Obviously, $I(\widehat{X}, \widehat{X}) = 1$, while the trajectories of \widehat{X} are naturally parameterised by the arc length.

Thus, every net has commutative representatives and unit representatives, which are normally different. The coincidence of these representatives characterises Chebyshev nets, see Proposition 4.1 (iii).

In what follows, we shall need some descriptors adopted from surface theory. Firstly,

$$\mathbf{n} = \frac{X_i\mathbf{r} \times X_j\mathbf{r}}{\sqrt{\|X_i\mathbf{r} \times X_j\mathbf{r}\|}}$$

are the unit normal vector to the supported surface. Secondly, the *fundamental coefficients* are defined by

$$I_{ij} = X_i\mathbf{r} \cdot X_j\mathbf{r}, \quad II_{ij} = X_jX_i\mathbf{r} \cdot \mathbf{n}. \quad (2.3)$$

These are analogues of the coefficients of the fundamental forms and coincide with them when $X_i = \partial/\partial x_i$ are the coordinate fields.

The expressions I_{ij}, II_{ij} are symmetric in i, j and invariant with respect to rigid motions. The symmetry of II_{ij} is obvious from $[X_i, X_j]\mathbf{r} \cdot \mathbf{n} = 0$.

3 Invariants of nets

Invariants of nets have been pioneered by Aoust [3] and Weise [93]. For an overview in various settings, see [28, 66, 74, 75, 76, 82]. For differential invariants in general, see [2]. Here we recall useful first- and second-order scalar differential invariants in terms of direction pairs. In fact, only five of the invariants, namely $\omega, K, \sigma, \pi_1, \pi_2$, will be essential for the main result of the paper, but for the sake of perspective we will review a larger set. Invariants of nets include, in particular, classical invariants of curves, surfaces, and curves on surfaces, which can be found in any textbook on classical differential geometry, in particular [83]. Relations among various invariants and the description how invariants change under five discrete symmetries can be found in Appendix A.

Given a direction pair $([X_1], [X_2])$, the scalar differential invariants of order $\leq r$ can be constructed from the Euclidean space metric and the derivatives $X_{i_s} \dots X_{i_1} \mathbf{r}$, $1 \leq s \leq r$, as expressions that are invariant with respect to rigid motions and multiplications (2.2). Higher-order scalar differential invariants can be obtained from lower-order ones by applying the invariant differentiations \widehat{X}_i (differentiations with respect to the arc length).

Following Sannia [71], expressions E satisfying $E' = f_1^{a_1} f_2^{a_2} E$ are called (a_1, a_2) -semiinvariants. Needless to say, invariants are synonymous to $(0, 0)$ -semiinvariants.

We start with invariants expressible in terms of the fundamental coefficients (2.3). Under $X'_i = f_i X_i$, the latter transform as

$$I'_{ij} = f_i f_j I_{ij}, \quad II'_{ij} = f_i f_j II_{ij}.$$

Consequently, I_{ij} and II_{ij} are $(\delta_{i1} + \delta_{j1}, \delta_{i2} + \delta_{j2})$ -semiinvariants, where δ_{ik} denotes the Kronecker symbol.

Observe that I_{ij} are of order 1, while II_{ij} are of order 2. According to the appendix, Table 2, there can be only one independent first-order invariant, for which we choose the non-oriented intersection angle ω determined by

$$\cos \omega = \frac{I_{12}}{\sqrt{I_{11} I_{22}}}, \quad \sin \omega = \sqrt{\frac{\det I}{I_{11} I_{22}}}$$

between 0 and π . The oriented intersection angle between 0 and 2π can be defined analogously, using $\sin \omega \mathbf{n} = \widehat{X}_1 \mathbf{r} \times \widehat{X}_2 \mathbf{r}$ to determine $\sin \omega$.

Associated with the surface S are two independent second-order invariants, for which we choose the Gauss and the mean curvature

$$K = \frac{\det II}{\det I}, \quad H = \frac{I_{11} II_{22} - 2I_{12} II_{12} + I_{22} II_{11}}{\det I}.$$

Associated with the curves of each family are the normal curvatures

$$nc_i = \frac{II_{ii}}{I_{ii}},$$

the geodesic curvatures

$$gc_i = \frac{[X_i \mathbf{r}, X_i X_i \mathbf{r}, \mathbf{n}]}{I_{ii}^{3/2}}$$

$([\mathbf{u}, \mathbf{v}, \mathbf{w}])$ denotes the triple product, i.e., the oriented volume of the parallelepiped spanned by the vectors $\mathbf{u}, \mathbf{v}, \mathbf{w}$, the ordinary curvatures $c_i = \sqrt{nc_i^2 + gc_i^2}$, and the geodesic torsions [94] or [54, p. 165]

$$gt_i = \frac{[X_i \mathbf{r}, \mathbf{n}, X_i \mathbf{n}]}{I_{ii}} = (-1)^i \frac{I_{12} II_{ii} - I_{ii} II_{12}}{I_{ii} \sqrt{\det I}}$$

(ordinary torsions and normal torsions are of order 3).

Of utmost importance for us is the *Schief curvature*

$$\sigma = \frac{X_2 X_1 \mathbf{r} \cdot \mathbf{n}}{\|X_1 \mathbf{r} \times X_2 \mathbf{r}\|} = \frac{[X_1 \mathbf{r}, X_2 \mathbf{r}, X_2 X_1 \mathbf{r}]}{[X_1 \mathbf{r}, X_2 \mathbf{r}, \mathbf{n}]^2} = \frac{II_{12}}{\sqrt{\det I}}, \quad (3.1)$$

introduced by W.K. Schief [78, Section 3.1] as a continuous limit of a curvature measure of discrete nets. Considering an infinitesimal tetrahedron spanned by the net, σ turns out to be proportional to the ratio of its volume to the squared area of its base, as well as to the ratio of its height to the area of its base, see loc. cit. for the details.

Remark 3.1. Obviously, conjugate nets are characterised by $\sigma = 0$, while the wobbly (“wackelige”) nets of Sauer [72] are characterised by admitting a σ -preserving isometry. Schief [78, Section 2.2] related Chebyshev nets of constant σ to the Pohlmeier–Lund–Regge system.

Next we consider invariants expressible in terms of I_{ij} and \widehat{X}_i . Firstly, for each $i = 1, 2$, the derivative

$$\omega_{,i} = \widehat{X}_i \omega$$

of the intersection angle with respect to the arc length is an invariant, matching the description of *courbure inclinée* by Aoust [3, I, Section 10].

Secondly, the commutation relation

$$[\widehat{X}_i, \widehat{X}_j] = \iota_j \widehat{X}_i + \iota_i \widehat{X}_j \quad (3.2)$$

can be taken for the definition of second-order invariants ι_i . One easily checks that

$$\iota_1 = \frac{\widehat{X}_2 I_{11}}{2 I_{11}}, \quad \iota_2 = -\frac{\widehat{X}_1 I_{22}}{2 I_{22}}.$$

More classical are Bortolotti curvatures [15, equations (1) and (2)], which can be introduced in the following way. Consider the covariant derivative $\nabla_{X_1} X_2$, defined by the property that $(\nabla_{X_1} X_2)\mathbf{r}$ is the projection of the vector $X_1 X_2 \mathbf{r}$ to the tangent space to S , at every point. Being tangent to the surface, $\nabla_{X_i} X_j$ can be expressed as a linear combination $\Gamma_{ij}^1 X_1 + \Gamma_{ij}^2 X_2$ of X_1, X_2 .^{2,3,4} By Cramer’s rule, explicit expressions for $\Gamma_{12}^1, \Gamma_{21}^2$ are

$$\Gamma_{12}^1 = \frac{1}{\det I} \begin{vmatrix} X_1 \mathbf{r} \cdot X_1 X_2 \mathbf{r} & X_1 \mathbf{r} \cdot X_2 \mathbf{r} \\ X_2 \mathbf{r} \cdot X_1 X_2 \mathbf{r} & X_2 \mathbf{r} \cdot X_2 \mathbf{r} \end{vmatrix}, \quad \Gamma_{21}^2 = \frac{1}{\det I} \begin{vmatrix} X_1 \mathbf{r} \cdot X_1 \mathbf{r} & X_1 \mathbf{r} \cdot X_2 X_1 \mathbf{r} \\ X_2 \mathbf{r} \cdot X_1 \mathbf{r} & X_2 \mathbf{r} \cdot X_2 X_1 \mathbf{r} \end{vmatrix}. \quad (3.3)$$

It is easily seen that Γ_{12}^1 is a $(0, 1)$ -semiinvariant, while Γ_{21}^2 is a $(1, 0)$ -semiinvariant. Hence,

$$\pi_1 = \frac{\Gamma_{12}^1}{\sqrt{I_{22}}}, \quad \pi_2 = \frac{\Gamma_{21}^2}{\sqrt{I_{11}}} \quad (3.4)$$

are invariants. Up to signs, $\pi_1 \sin \omega, \pi_2 \sin \omega$ coincide with the aforementioned Bortolotti curvatures [15, equations (1) and (2)]. Related to them are also the Chebyshev curvature and the Chebyshev vector, see [93] and [82, Section 23], which we omit.

4 Chebyshev nets

Originally introduced to model woven fabrics conforming to a body [19, 35], Chebyshev nets have important applications and are subject to active research till today [26, 41, 62, 70]. As the most exciting architectural application, Chebyshev nets model elastic timber structures (gridshells) obtained by buckling a flat straight rectangular grid connected by joints [52]. A manifestly invariant characterisation of Chebyshev nets is the *curvilinear parallelogram condition* (opposite sides of curvilinear quadrilaterals formed by pairs of curves of each family have the same length), see Bianchi [9, Section 379] or Darboux [25, Section 642].

Proposition 4.1. *The following statements about a net and the corresponding direction pair $([X_1], [X_2])$ are equivalent:*

²If $X_i = \partial/\partial x_i$, then Γ_{ij}^k become the usual Christoffel symbols.

³Contrary to Christoffel symbols, $\Gamma_{ij}^k \neq \Gamma_{ji}^k$ in general.

⁴By the way, $\Gamma_{21}^1, \Gamma_{12}^2$ are not semiinvariants, while $\Gamma_{11}^2, \Gamma_{22}^1$ are related to the geodesic curvatures, see [15].

(i) the family parameters x, y can be chosen in such a way that the first fundamental form is

$$dx^2 + 2 \cos \omega dx dy + dy^2 \quad (4.1)$$

(the Chebyshev parameterisation; ω coincides with the intersection angle invariant);

(ii) all unit vectors in one direction of the net are parallel along all curves in the other direction, i.e.,

$$\nabla_{X_1} \widehat{X}_2 = 0, \quad \nabla_{X_2} \widehat{X}_1 = 0$$

(see Bianchi [10]);

(iii) the unit representatives commute, i.e.,

$$[\widehat{X}_1, \widehat{X}_2] = 0;$$

(iv) the invariants ι_i vanish, that is,

$$\iota_1 = 0 = \iota_2, \quad \text{i.e.,} \quad X_2 \mathbf{I}_{11} = 0 = X_1 \mathbf{I}_{22};$$

(v) the Bortolotti curvatures (3.4) vanish, that is,

$$\pi_1 = 0 = \pi_2;$$

(vi) the geodesic curvatures satisfy

$$\text{gc}_1 = -\widehat{X}_1 \omega, \quad \text{gc}_2 = \widehat{X}_2 \omega$$

(see [61, equation (4.7)]).

Proof. (i) \Rightarrow (ii). If (i) holds, then both $\partial/\partial x$ and $\partial/\partial y$ are unit vectors. The Bianchi condition (ii) can be verified by the straightforward calculation of the covariant derivatives.

(ii) \Rightarrow (iii). If (ii) holds, then $[\widehat{X}_1, \widehat{X}_2] = \nabla_{\widehat{X}_1} \widehat{X}_2 - \nabla_{\widehat{X}_2} \widehat{X}_1 = 0$.

(iii) \Rightarrow (i). If (iii) holds, then one can choose coordinates x, y in such a way that $\partial/\partial x = \widehat{X}_1$ and $\partial/\partial y = \widehat{X}_2$. Being equal to the squared lengths of the vectors $\widehat{X}_i \mathbf{r}$, the metric coefficients at dx^2 and dy^2 are equal to 1.

(iii) \Leftrightarrow (iv) is obvious by formula (3.2), which defines ι_i .

(iv) \Leftrightarrow (v) is obvious from identities (A.3) in Appendix A.

(v) \Leftrightarrow (vi) is obvious from identities (A.2) in Appendix A. ■

Remark 4.2. Another criterion is the vanishing of the Chebyshev vector [66, Section 67] or [82, Section 55]. Yet different criteria can be found in [37, 70, 78, 92].

Remark 4.3. Associated with every Chebyshev parameterisation (4.1) is the *isodiagonal* parameterisation ([90, Section 1] or [25, Section 678]) by $u = x + y$, $v = x - y$. In terms of u, v , the metric is

$$\mathbf{I} = \cos^2 \frac{1}{2} \omega du^2 + \sin^2 \frac{1}{2} \omega dv^2.$$

5 Integrable nets

The literature on soliton geometries is very extensive, but authors (except [84]) seem reluctant to define them in any other way than by means of examples. In this section we attempt to give a definition, which covers both surfaces and nets (Definition 5.1).

Integrability is understood in the conventional sense of soliton theory [11, 39, 69, 84]. The integrability criterion is the existence of a zero-curvature representation (ZCR) [96]

$$D_y A - D_x B + [A, B] = 0,$$

where, firstly, A, B are elements of a finite-dimensional and non-solvable matrix Lie algebra that cannot be reduced to a solvable one by gauge transformations and, secondly, A, B depend on a (spectral) parameter that is not removable by gauge transformation. A gauge transformation by means of a gauge matrix H is the correspondence

$$A' = D_x H \cdot H^{-1} + H \cdot A \cdot H^{-1}, \quad B' = D_y H \cdot H^{-1} + H \cdot B \cdot H^{-1}.$$

For simple criteria of reducibility and removability, see [59, 60].

For both surfaces and nets, we require integrability of the Gauss–Mainardi–Codazzi system. The system is, in compact form [83, 84],

$$R_{ijkl} = \Pi_{jk}\Pi_{il} - \Pi_{ik}\Pi_{jl}, \quad \Pi_{ij;k} = \Pi_{ik;j} \quad (5.1)$$

(R_{ijkl} is the Riemann tensor and the semicolon denotes the covariant derivatives). We also recall that the Gauss–Mainardi–Codazzi equations are the compatibility conditions of the Gauss–Weingarten system

$$\mathbf{r}_{,ij} = \Gamma_{ij}^k \mathbf{r}_{,k} + \Pi_{ij} \mathbf{n}, \quad \mathbf{n}_{,i} = \Pi_i^k \mathbf{r}_{,k}, \quad (5.2)$$

which describes the immersed surfaces and their normals (Γ_{ij}^k are the Christoffel symbols and the index k in Π_i^k is raised by the metric I_{ij}). In expanded form, the Gauss–Mainardi–Codazzi system consists of three partial differential equations on six unknowns I_{ij} , Π_{ij} , and can be found in all standard textbooks on surface geometry.

Besides integrability, another key point is the geometric characterisability of the class. The three partial differential equations on six unknowns can be supplemented with as much as three other conditions (or more if auxiliary functions are introduced). Normally, two conditions (usually algebraic) are spent on specifying a particular parameterisation, leaving room for one condition to characterise the class.

To characterise a geometric class of surfaces (nets) in Euclidean space, the condition must be invariant with respect to Euclidean motions and arbitrary reparameterisations of surfaces (nets). In other words, there must exist a formulation of the condition in terms of differential invariants of surfaces (nets), at least in principle. Therefore, it seems natural to define integrable classes in the following way, suitable for specifying classification problems.

Definition 5.1. A class of surfaces (nets) is called *integrable* if it can be determined by a condition written in terms of differential invariants of surfaces (nets) and the Gauss–Mainardi–Codazzi system augmented with this condition is integrable in an appropriate parameterisation.

Proposition 5.2. *If a class of nets is integrable, then so is the class of supported surfaces.*

Proof. Obvious from the definition. ■

The appropriate parameterisation the definition refers to should exist for every member of the class. Its purpose is to make the whole system determined. For instance, the parameterisation may be principal for generic surfaces, asymptotic for hyperbolic surfaces, Chebyshev for Chebyshev nets, etc. However, experience shows that if a system is integrable in one parameterisation, then it is integrable in any other, even in a general one (in which case the whole system is underdetermined). This may be related to the fact that the zero curvature representation is also a geometric notion, which can be understood as a matrix-Lie-algebra-valued 1-form $\alpha = A dx + B dy$ satisfying $d\alpha = \frac{1}{2}[\alpha, \alpha]$, and the gauge transformation as $\alpha' = dH \cdot H^{-1} + H \cdot \alpha \cdot H^{-1}$.

Integrable classes of nets have been with us since the dawn of differential geometry of surfaces. For principal conformal nets, see Remark 5.3 below. To name others, conjugate nets are connected with the Laplace–Darboux integrability [23, 47]. Moreover, classical integrable geometries include integrable curve evolutions [40, 50, 65, 69, 79], which form integrable nets if completed with the evolution trajectories. Furthermore, integrable foliations of surfaces by curves [20, 77, 86] can be completed to integrable nets by the orthogonal curves. Apparently, already a review of the known cases would be a formidable task, not speaking about their invariant characterisations.

A systematic search for integrable classes of nets can be performed in the same manner as the search for integrable classes of surfaces. A natural way is to incorporate a non-removable spectral parameter into the $\mathfrak{so}(3)$ -valued zero-curvature representation induced by the Gauss–Weingarten system [84], either by the symmetry method [21, 51, 18] or by the more powerful cohomological method [4].

It is worth mentioning that classification results for integrable nets may also include integrable surfaces equipped with the nets in question. For example, linear Weingarten surfaces appeared in the classification of integrable classes of Chebyshev parameterisations⁵ in [48, Section 2].

Remark 5.3. Integrable classes of nets and integrable classes of surfaces mutually correspond (think of the class of all surfaces capable of carrying the nets). Therefore, classification of integrable surfaces and classification of integrable nets are interrelated, but in a complicated way.

For instance, isothermic surfaces and principal conformal nets (meaning nets generated by principal conformal parameterisations) [22, 87] determine each other uniquely and the study of isothermic surfaces is the same thing as the study of principal conformal nets. It can be easily seen that principal nets are characterised by the vanishing of $\cos \omega$ and either of σ , gt_1 , gt_2 , which are of order 1 and 2, respectively, whereas conformal nets are characterised by the vanishing of $\cos \omega$ and $\widehat{X}_1 gc_1 + \widehat{X}_2 gc_2$, which are of order 1 and 3, respectively. On the other hand, the lowest-order nontrivial surface invariant vanishing for all isothermic surfaces is $(k_1 - 2k_2)_{,12} + (k_2 - 2k_1)_{,21}$, which is of order 4 (k_i are the principal curvatures and comma denotes differentiation with respect to the arc length in principal directions). Therefore, principal conformal nets appear earlier (at lower order) in the classification of nets than isothermic surfaces in the classification of surfaces.

As a rule, if a net is integrable, then so are the various *derived* nets (on the same or another surface) obtained by geometric constructions. Thus, a complete classification of integrable classes (to a certain order of invariants), if such a goal were achievable, would consist of a rather complex interconnected (and infinite) network. However, invariant description of many derived nets will be of higher order than that of the net they are derived from, often far out of reach of presently available classification methods. Classification efforts will most likely spot only the integrable classes on the “border”, while the derived nets will allow to penetrate deeper into the “integrable region”.

⁵Integrable classes of parameterisations can be introduced by Definition 5.1 stripped of the invariance requirement.

Let us, finally, remark that one may also look for integrable parameterisations of a given surface, requiring the integrability of the system to obtain such a parametrisation (for instance, the Servant equations, see in the beginning of the next section). This is, however, a different problem.

6 Integrable Chebyshev nets

Voss [90] obtained large classes of explicit Chebyshev nets, among others on surfaces of revolution; he also proved that Chebyshev nets on the sphere correspond to solutions of the sine-Gordon equation [90, Section 3]. For pictures, see [41, 57]; the work [41] also addresses Chebyshev nets of class C^1 . Given a surface metric, obtaining general Chebyshev nets is possible by solving the Servant equations [80, equation (3)], which are, however, not always integrable. Integrable are also special Chebyshev nets that can be found according to [78, Section 2.2], cf. Remark 3.1.

In the earlier paper [48, Section 2], we looked for integrable Gauss–Mainardi–Codazzi systems in Chebyshev parameterisation. Our result consisted of five classes,⁶ including Case 2 specified by the linear relation

$$\mu K + \kappa \frac{\Pi_{12}}{\sin \omega} + \lambda = 0, \quad (6.1)$$

where μ , κ , λ are real constants, K is the Gauss curvature, Π_{12} is the coefficient of the second fundamental form with respect to the Chebyshev parameterisation, and ω is the intersection angle. As the parameterisation-dependent term $\Pi_{12}/\sin \omega$ in formula (6.1) coincides with the Schief curvature (3.1) (since Chebyshev parameterisations satisfy $I_{11} = 1 = I_{22}$), we see that condition (6.1) can be rewritten as

$$\mu K + \kappa \sigma + \lambda = 0, \quad (6.2)$$

where μ , κ , λ are arbitrary constants. Manifestly, condition (6.2) specifies a geometric class of nets. We already know from [48] that the corresponding Gauss–Mainardi–Codazzi system is integrable (has a ZCR). Hence, condition (6.2) determines an integrable class of nets according to Definition 5.1.

Topologically, the “space” of conditions $\mu K + \kappa \sigma + \lambda = 0$ is the projective space $\mathbb{R}P^2$ (a sphere with identified antipodal points), see Figure 1. The discrete symmetries T_{-1}, \dots, T_2 (see Table 5 in the appendix) change the sign of σ , that is, the sign of κ , identifying $\mu K + \kappa \sigma + \lambda = 0$ with $\mu K - \kappa \sigma + \lambda = 0$.

Remark 6.1. When at least one of μ , κ is zero, the Chebyshev nets satisfying condition (6.2) fall into one of the following classes:

1. If $\kappa = 0$, $\mu \neq 0$ (the green circle in Figure 1), then condition (6.2) implies the constancy of K . Thus, we arrive at surfaces of constant Gaussian curvature equipped with an arbitrary Chebyshev net, including developable surfaces (the intersection of green and white circle).
2. If $\mu = 0$ and $\kappa \neq 0$ (the yellow circle in Figure 1), then condition (6.2) implies the constancy of the Schief curvature σ , which is the situation explored in Schief [78, Section 2.2]. One obtains the equation $\mathbf{r}_{xy} = \sigma \mathbf{r}_x \cdot \mathbf{r}_y$, identifiable with the integrable Lund–Regge system. For finite-gap solutions, see Shin [81]. If, moreover, $\lambda = 0$ (the intersection of yellow and white circle), then $\sigma = 0$. This yields the well-understood class of translation surfaces [23, Sections 81 and 82], i.e., solutions of the equation $\mathbf{r}_{xy} = 0$.

⁶Chebyshev nets on linear Weingarten surfaces have been studied in [56].

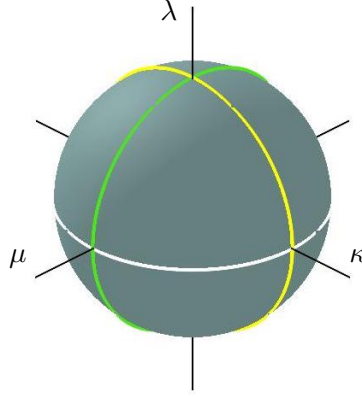


Figure 1. The space of conditions $\mu K + \kappa\sigma + \lambda = 0$. Antipodal points coincide.

We see that the cases of $\mu = 0$ or $\kappa = 0$ (the green and the yellow circle) have already been sufficiently understood. Therefore, we may assume that $\mu \neq 0 \neq \kappa$ in what follows. Dividing condition (6.2) by $\mu \neq 0$ is equivalent to setting $\mu = 1$, which we assume henceforth.

Remark 6.2. Using identities listed in Appendix A, condition (6.2) can be rewritten in different ways, for instance

$$\frac{nc_1^2 + gt_1^2 - \kappa gt_1 - \lambda}{nc_1} = \frac{nc_2^2 + gt_2^2 + \kappa gt_2 - \lambda}{nc_2}$$

(a relation between two curve invariants on the surface) or

$$\cot \omega + \cot \omega_{\text{III}} = -2H \frac{K + \lambda}{\kappa K}$$

(a relation among two angle invariants and a surface invariant).

From now on, until otherwise stated, we use the Chebyshev parameterisation, i.e., we consider the first fundamental form (4.1), leaving the second fundamental form arbitrary. We assume that $\sin \omega \neq 0$ henceforth, i.e., we assume that all points are nonsingular in the sense of Definition 2.1.

Let us introduce variables h_{ij} by

$$\Pi_{ij} = h_{ij} \sin \omega.$$

In terms of h_{ij} , the Gauss and the Schief curvatures are simply

$$K = h_{11}h_{22} - h_{12}^2 = \det h, \quad \sigma = h_{12},$$

while condition (6.2) becomes

$$\mu(h_{11}h_{22} - h_{12}^2) + \kappa h_{12} + \lambda = 0. \quad (6.3)$$

The Gauss–Weingarten system is

$$\begin{aligned} \mathbf{r}_{xx} &= h_{11} \sin \omega \mathbf{n} + \omega_x \cot \omega \mathbf{r}_x - (\omega_x / \sin \omega) \mathbf{r}_y, \\ \mathbf{r}_{xy} &= h_{12} \sin \omega \mathbf{n}, \\ \mathbf{r}_{yy} &= h_{22} \sin \omega \mathbf{n} + \omega_y \cot \omega \mathbf{r}_y - (\omega_y / \sin \omega) \mathbf{r}_x, \\ \mathbf{n}_x &= \frac{h_{12} \cos \omega - h_{11}}{\sin \omega} \mathbf{r}_x + \frac{h_{11} \cos \omega - h_{12}}{\sin \omega} \mathbf{r}_y, \\ \mathbf{n}_y &= \frac{h_{22} \cos \omega - h_{12}}{\sin \omega} \mathbf{r}_x + \frac{h_{12} \cos \omega - h_{22}}{\sin \omega} \mathbf{r}_y, \end{aligned} \quad (6.4)$$

the Gauss–Mainardi–Codazzi equations (the compatibility conditions of the Gauss–Weingarten system) being

$$\begin{aligned}\omega_{xy} + K \sin \omega &= 0, \\ h_{11,y} &= h_{12,x} - h_{11}\omega_y \cot \omega + h_{22}\omega_x/\sin \omega, \\ h_{12,y} &= h_{22,x} - h_{11}\omega_y/\sin \omega + h_{22}\omega_x \cot \omega.\end{aligned}\tag{6.5}$$

These systems should be completed with condition (6.3). We do this by solving (6.3) for h_{22} and inserting

$$h_{22} = \frac{\mu h_{12}^2 - \kappa h_{12} - \lambda}{\mu h_{11}}\tag{6.6}$$

into (6.4) and (6.5).

7 Vector conservation laws

In this section, we look for vector conservation laws of the form $\mathbf{P} dx + \mathbf{Q} dy$, where \mathbf{P} , \mathbf{Q} are linear combinations of \mathbf{r}_x , \mathbf{r}_y , \mathbf{n} such that

$$D_y \mathbf{P} - D_x \mathbf{Q} = 0$$

holds as a consequence of the Gauss–Mainardi–Codazzi equations (6.5) and the Gauss–Weingarten equations (6.4) under condition (6.2). For every vector conservation law, we define the associated vector potential \mathbf{w} to be a vector satisfying $d\mathbf{w} = \mathbf{P} dx + \mathbf{Q} dy$, that is, $\mathbf{w}_x = \mathbf{P}$, $\mathbf{w}_y = \mathbf{Q}$. The vector conservation law is said to be trivial if the corresponding potential \mathbf{w} can be found among the local functions as a linear combination of \mathbf{r}_x , \mathbf{r}_y , \mathbf{n} , the coefficients being functions of x , y , ω , h_{11} , h_{12} and their derivatives.

Finding vector conservation laws is no harder than finding scalar ones. In our case, the main obstacle is that the Gauss–Weingarten system is overdetermined and, therefore, we cannot use the correspondence between conservation laws and cosymmetries. Wolf’s [95] comparison of four approaches to computation of conservation laws indicates that the method that is most likely to lead to an answer, is the following (the third) one.

Let $W_i = 0$, $i = 1, \dots, 3$, be individual equations of the Gauss–Mainardi–Codazzi system (6.5) and $\mathbf{W}_i = 0$, $i = 1, \dots, 5$, individual equations of the Gauss–Weingarten system (6.4). For further reference,

$$\begin{aligned}W_2 &= -h_{11,y} + h_{12,x} - h_{11}\omega_y \cot \omega + h_{22}\omega_x/\sin \omega, \\ W_3 &= -h_{12,y} + h_{22,x} - h_{11}\omega_y/\sin \omega + h_{22}\omega_x \cot \omega, \\ \mathbf{W}_1 &= -\mathbf{r}_{xx} + h_{11} \sin \omega \mathbf{n} + \omega_x \cot \omega \mathbf{r}_x - (\omega_x/\sin \omega) \mathbf{r}_y, \\ \mathbf{W}_2 &= -\mathbf{r}_{xy} + h_{12} \sin \omega \mathbf{n}, \\ \mathbf{W}_3 &= -\mathbf{r}_{yy} + h_{22} \sin \omega \mathbf{n} + \omega_y \cot \omega \mathbf{r}_y - (\omega_y/\sin \omega) \mathbf{r}_x,\end{aligned}$$

(we omit W_1 , \mathbf{W}_4 and \mathbf{W}_5 , which we shall not need explicitly). Then we can write

$$D_y \mathbf{P} - D_x \mathbf{Q} = \sum \mathbf{C}_i W_i + \sum C_i \mathbf{W}_i,$$

for suitable characteristics \mathbf{C}_1 , \mathbf{C}_2 , \mathbf{C}_3 and C_1, \dots, C_5 . Applying the Euler–Lagrange operator

$$\frac{\delta}{\delta z} = \sum_J (-D)_J \frac{\partial}{\partial z}$$

with z running through all dependent variables $z = \mathbf{r}, \mathbf{n}, \omega, h_{11}, h_{12}$, we get

$$0 = \sum_J (-D)_J \frac{\partial}{\partial z} \left(\sum C_i W_i + \sum C_i \mathbf{W}_i \right), \quad z = \mathbf{r}, \mathbf{n}, \omega, h_{11}, h_{12}. \quad (7.1)$$

These are five equations on the eight unknowns $\mathbf{C}_1, \mathbf{C}_2, \mathbf{C}_3, C_1, \dots, C_5$. Three ignorable solutions correspond to the trivial conservation laws $d\mathbf{n}, d\mathbf{r}_x, d\mathbf{r}_y$. A non-ignorable solution to (7.1) is

$$\begin{aligned} C_1 &= h_{22}, & \mathbf{C}_1 &= 0, \\ C_2 &= 2\kappa - 2h_{12}, & \mathbf{C}_2 &= \mathbf{r}_y, \\ C_3 &= h_{11}, & \mathbf{C}_3 &= -\mathbf{r}_x, \end{aligned}$$

valid if and only if $\lambda = 0$. This leads us to the following proposition.

Proposition 7.1. *Assuming $\sin \omega \neq 0$, expressions*

$$\mathbf{P} = (h_{12} - \kappa) \mathbf{r}_x - h_{11} \mathbf{r}_y, \quad \mathbf{Q} = h_{22} \mathbf{r}_x + (\kappa - h_{12}) \mathbf{r}_y$$

are components of a vector conservation law if and only if $\lambda = 0$.

Proof. It is straightforward to check that $D_y \mathbf{P} - D_x \mathbf{Q} = 2\lambda \sin \omega \mathbf{n}$, which is zero if and only if $\lambda = 0$. ■

The vanishing of λ (the white circle in Figure 1) means that the Schief curvature σ is proportional to the Gauss curvature K . After the concordance of the two measures, we introduce the following terminology (applicable to arbitrary nets, non necessarily Chebyshev ones).

Definition 7.2. Nets satisfying $K = \kappa\sigma$, $\kappa \in \mathbb{R}$, will be called *concordant nets*.

By Remark 6.2 and formula (A.5), an equivalent formulation of concordance is

$$\cot \omega_{\text{III}} + \cot \omega = -2H/\kappa.$$

8 From concordant nets to pairs of pseudospherical surfaces

In this section, x, y continue to denote the Chebyshev parameters.

Following Proposition 7.1, let \mathbf{m} denote the vector potential satisfying

$$\begin{aligned} \mathbf{m}_x &= (h_{12} - \kappa) \mathbf{r}_x - h_{11} \mathbf{r}_y, \\ \mathbf{m}_y &= h_{22} \mathbf{r}_x + (\kappa - h_{12}) \mathbf{r}_y. \end{aligned} \quad (8.1)$$

The vector \mathbf{m} is crucial in what follows.

Definition 8.1. We define the *associated surfaces* S^+, S^- of a concordant net by the parameterisations

$$\mathbf{r}^+ = \mathbf{r} + \mathbf{m}/\kappa, \quad \mathbf{r}^- = \mathbf{r} - \mathbf{m}/\kappa. \quad (8.2)$$

Theorem 8.2. *Consider a concordant Chebyshev net satisfying $K = \kappa\sigma$. Then*

- (i) *the associated surfaces $\mathbf{r}^+, \mathbf{r}^-$ are regular wherever $\sigma \neq 0$ and $\sin \omega \neq 0$;*
- (ii) *$\mathbf{r}^+, \mathbf{r}^-$ are pseudospherical of the Gauss curvature $-\kappa^2$;*
- (iii) *all three surfaces $\mathbf{r}^+, \mathbf{r}^-, \mathbf{r}$ have one and the same normal vector \mathbf{n} at the corresponding points;*

(iv) assuming that x, y are Chebyshev parameters, $[\partial/\partial x]$ and $[\partial/\partial y]$ are asymptotic directions for \mathbf{r}^+ and \mathbf{r}^- , respectively.

Proof. Obviously from formulas (8.1) and (8.2), \mathbf{n} is orthogonal to both \mathbf{r}_x^\pm and \mathbf{r}_y^\pm , and the third statement follows.

Computing the components of the corresponding fundamental forms I^\pm and II^\pm , we get

$$\begin{aligned}\kappa^2 I_{11}^+ &= h_{11}^2 - 2 \cos \omega h_{11} h_{12} + h_{12}^2, \\ \kappa^2 I_{12}^+ &= h_{11}(h_{12} - 2\kappa) - 2 \cos \omega h_{12}(h_{12} - \frac{3}{2}\kappa) + h_{12} h_{22}, \\ \kappa^2 I_{22}^+ &= (h_{12} - 2\kappa)^2 - 2 \cos \omega (h_{12} - 2\kappa) h_{22} + h_{22}^2\end{aligned}$$

and, symmetrically,

$$\begin{aligned}\kappa^2 I_{11}^- &= h_{11}^2 - 2 \cos \omega (h_{12} - 2\kappa) h_{11} + (h_{12} - 2\kappa)^2, \\ \kappa^2 I_{12}^- &= h_{11} h_{12} - 2 \cos \omega h_{12}(h_{12} - \frac{3}{2}\kappa) + (h_{12} - 2\kappa) h_{22}, \\ \kappa^2 I_{22}^- &= h_{12}^2 - 2 \cos \omega h_{12} h_{22} + h_{22}^2.\end{aligned}$$

Then $\det I^\pm = (\sigma/\kappa)^2 \sin^2 \omega$ is nonzero wherever $\sigma \neq 0$ and $\sin \omega \neq 0$, which proves the first statement.

Concerning II^\pm we have

$$\begin{aligned}II_{11}^+ &= 0, & II_{12}^+ &= \sin \omega h_{12}, & II_{22}^+ &= 2 \sin \omega h_{22}, \\ II_{11}^- &= -2 \sin \omega h_{11}, & II_{12}^- &= -\sin \omega h_{12}, & II_{22}^- &= 0.\end{aligned}$$

The vanishing of II_{11}^+ and II_{22}^- reveals the asymptotic directions $\partial/\partial x$ and $\partial/\partial y$, which proves the fourth statement.

Using equation (6.2)| $_{\lambda=0}$, we get

$$K^+ = \frac{\det II^+}{\det I^+} = -\kappa^2, \quad K^- = \frac{\det II^-}{\det I^-} = -\kappa^2,$$

which proves the second statement. ■

To equip the surfaces S^+ , S^- with the asymptotic Chebyshev parameterisations, we employ the mean curvatures, which are easily seen to be

$$H^+ = \frac{h_{12} \sin \omega}{h_{12} \cos \omega - h_{11}}, \quad H^- = \frac{h_{12} \sin \omega}{h_{22} - h_{12} \cos \omega}. \quad (8.3)$$

Here and in what follows, $h_{22} = (h_{12}^2 - \kappa h_{12})/h_{11}$ by formula (6.6).

Proposition 8.3. Denote

$$\varphi^+ = -\arctan \frac{\kappa}{H^+}, \quad \varphi^- = \arctan \frac{\kappa}{H^-},$$

where H^+ and H^- are given by formulas (8.3). Let $\xi^- = x$, $\eta^+ = y$. In the notation from the proof of Theorem 8.2, define ξ^+ and η^- by compatible equations

$$\xi_x^+ = \sqrt{I_{11}^+} = \frac{1}{\kappa} \sqrt{h_{11}^2 - 2h_{11}h_{12} \cos \omega + h_{12}^2}, \quad \xi_y^+ = \frac{h_{22}}{h_{12}} \xi_x^+ \quad (8.4)$$

and

$$\eta_x^- = \frac{h_{11}}{h_{12}} \eta_y^-, \quad \eta_y^- = \sqrt{II_{22}^-} = \frac{1}{\kappa} \sqrt{h_{12}^2 - 2h_{12}h_{22} \cos \omega + h_{22}^2}, \quad (8.5)$$

respectively. Then ξ^+ , η^+ and ξ^- , η^- are the corresponding asymptotic Chebyshev parameters on \mathbf{r}^+ and \mathbf{r}^- , while ϕ^+ and ϕ^- are the corresponding Chebyshev angles.

Proof. One can check that systems (8.4) and (8.5) are indeed compatible and

$$\begin{aligned} I^\pm &= (d\xi^\pm)^2 + 2 \cos \phi^\pm d\xi^\pm d\eta^\pm + (d\eta^\pm)^2, \\ \text{II}^\pm &= \pm 2\kappa \sin \phi^\pm d\xi^\pm d\eta^\pm \end{aligned}$$

by straightforward computation. This implies both statements. \blacksquare

Corollary 8.4. *In the notation from Proposition 8.3,*

$$\phi_{\xi^\pm \eta^\pm}^\pm = \kappa^2 \sin \phi^\pm,$$

meaning that $\phi^\pm(\xi^\pm, \eta^\pm)$ are solutions of the sine-Gordon equation.

Proposition 8.5. *In the notation from Proposition 8.3, the coordinate vector fields corresponding to ξ^\pm, η^\pm are*

$$\begin{aligned} D_{\xi^+} &= \frac{\kappa}{\sqrt{h_{11}^2 - 2h_{11}h_{12} \cos \omega + h_{12}^2}} D_x, & D_{\eta^+} &= -\frac{h_{22}}{h_{12}} D_x + D_y, \\ D_{\xi^-} &= D_x - \frac{h_{11}}{h_{12}} D_y, & D_{\eta^-} &= \frac{\kappa}{\sqrt{h_{12}^2 - 2h_{12}h_{22} \cos \omega + h_{22}^2}} D_y. \end{aligned}$$

Proof. By straightforward verification of $D_{\xi^\pm} \xi^\pm = 1$, $D_{\xi^\pm} \eta^\pm = 0$, $D_{\eta^\pm} \xi^\pm = 0$, $D_{\eta^\pm} \eta^\pm = 1$, and $[D_{\xi^\pm}, D_{\eta^\pm}] = 0$. \blacksquare

It is well known that the asymptotic Chebyshev net on a pseudospherical surface induces a Chebyshev net on the Gauss sphere (and vice versa). Consequently, the pair \mathbf{r}^\pm induces a pair of such nets. Their relative position depends on the angle ω in a very simple way.

Proposition 8.6. *In the notation from Proposition 8.5,*

- (i) *the fields $D_{\xi^\pm}, D_{\eta^\pm}$ induce a pair of Chebyshev nets on the unit sphere;*
- (ii) *the oriented angle $\angle(D_{\xi^-} \mathbf{n}, D_{\eta^+} \mathbf{n})$ equals $\pi + \omega$.*

Proof. The tangent vectors to the Gauss sphere are

$$\begin{aligned} D_{\xi^+ \mathbf{n}} &= \frac{\kappa}{\sin \omega} \frac{(h_{11} - h_{12} \cos \omega) \mathbf{r}_x + (h_{11} \cos \omega - h_{12}) \mathbf{r}_y}{\sqrt{h_{11}^2 - 2h_{11}h_{12} \cos \omega + h_{12}^2}}, \\ D_{\eta^+ \mathbf{n}} &= \frac{\kappa}{\sin \omega} (\cos \omega \mathbf{r}_y - \mathbf{r}_x), \\ D_{\xi^- \mathbf{n}} &= \frac{\kappa}{\sin \omega} (\cos \omega \mathbf{r}_x - \mathbf{r}_y), \\ D_{\eta^+ \mathbf{n}} &= \frac{\kappa}{\sin \omega} \frac{(h_{22} - h_{12} \cos \omega) \mathbf{r}_y + (h_{22} \cos \omega - h_{12}) \mathbf{r}_x}{\sqrt{h_{12}^2 - 2h_{12}h_{22} \cos \omega + h_{22}^2}}. \end{aligned}$$

Statement (i) is easily verified by checking the identities

$$D_{\xi^+ \mathbf{n}} \cdot D_{\xi^+ \mathbf{n}} = D_{\xi^- \mathbf{n}} \cdot D_{\xi^- \mathbf{n}} = D_{\eta^+ \mathbf{n}} \cdot D_{\eta^+ \mathbf{n}} = D_{\eta^- \mathbf{n}} \cdot D_{\eta^- \mathbf{n}} = \kappa^2.$$

Let ψ denote the oriented angle $\angle(D_{\xi^-} \mathbf{n}, D_{\eta^+} \mathbf{n})$. To prove (ii), one easily computes

$$\cos \psi = \frac{D_{\xi^-} \mathbf{n} \cdot D_{\eta^+} \mathbf{n}}{\kappa^2} = -\cos \omega,$$

and

$$\sin \psi \mathbf{n} = \frac{D_{\xi^-} \mathbf{n} \times D_{\eta^+} \mathbf{n}}{\kappa^2} = -\sin \omega \mathbf{n}.$$

Therefore, $\psi = \pi + \omega$. \blacksquare

Finally, it is easy to check the Lelievre formulas [69, equation (1.140)]

$$D_{\xi^\pm} \mathbf{r}^\pm = -\frac{1}{\kappa} D_{\xi^\pm} \mathbf{n} \times \mathbf{n}, \quad D_{\eta^\pm} \mathbf{r}^\pm = \frac{1}{\kappa} D_{\eta^\pm} \mathbf{n} \times \mathbf{n},$$

which relate the pseudospherical surfaces \mathbf{r}^\pm to their Gauss images.

9 From pairs of pseudospherical surfaces to concordant nets

In this section, we prove the converse of Theorem 8.2. Given a pair of pseudospherical surfaces of equal constant negative Gaussian curvatures, we construct the corresponding concordant Chebyshev net. We draw inspiration from the results of the previous section, but the proofs have very little in common.

We denote surfaces differently from the previous section. This is not only more convenient for the proof of Theorem 9.3, but it also helps to separate the two proofs. The reader may wish to consult Table 1 for important matches and differences. Note that many concepts have no counterpart in the previous section and vice versa.

Previous section	This section
\mathbf{n}	\mathbf{n}
$\mathbf{r}, \mathbf{r}^+, \mathbf{r}^-$	$\bar{\mathbf{r}}, \mathbf{r}, \mathbf{r}'$
x, y, ξ^\pm, η^\pm	nothing
nothing	p, q, ξ, η
$D_{\xi^\pm}, D_{\eta^\pm}$	\widehat{X}_i for various ε_i

Table 1. Translation table between Sections 8 and 9.

The key idea drawn from the previous section is the parallelism induced by the coincidence of normal vectors.

Definition 9.1. The *parallelism* [31, 36, 67] between two surfaces S, S' is a correspondence between S and S' such that the diagram

$$\begin{array}{ccc}
 S & \xleftrightarrow{\text{parallelism}} & S' \\
 \searrow \gamma & & \swarrow \gamma' \\
 & \mathbb{S}^2 &
 \end{array} \tag{9.1}$$

is commutative. Here \mathbb{S}^2 is the unit sphere, while γ, γ' denote the Gauss maps.

Obviously by the definition of the Gauss map, the surfaces S, S' have equal normals and equal tangent planes at corresponding points. This is why the parallelism is also known as the *parallelism of normals* or the *parallelism of tangent planes*.

The parallelism implies the possibility to establish local parameterisations $\mathbf{r}, \mathbf{r}': U \rightarrow \mathbf{E}^3$ that complete the commutative diagram (9.1) into

$$\begin{array}{ccc}
 & U & \\
 \mathbf{r} \swarrow & & \searrow \mathbf{r}' \\
 S & \xleftrightarrow{\text{parallelism}} & S' \\
 \searrow \gamma & & \swarrow \gamma' \\
 & \mathbb{S}^2 &
 \end{array}$$

whenever $\text{Im } \gamma$ intersects with $\text{Im } \gamma'$. Such maps \mathbf{r}, \mathbf{r}' will be referred to as *parallel parameterisations*. They are not unique since they can be combined with an arbitrary diffeomorphism $U \rightarrow U$.

To put it simply, $\mathbf{n} = \gamma \circ \mathbf{r} = \gamma' \circ \mathbf{r}' = \mathbf{n}'$ as maps $U \rightarrow \mathbb{S}^2$. For generic surfaces, γ, γ' are local diffeomorphisms. If this is the case, parallel parameterisations locally exist. However, the Gauss maps need not be global diffeomorphisms (for a wealth of beautiful examples, see [16]).

Definition 9.2. Consider a pair of surfaces S, S' . The locus \bar{S} of mid-points between points related by parallelism is called the *middle surface*.

More explicitly, if $\mathbf{r}(p, q), \mathbf{r}'(p, q)$ are parallel local parameterisations of surfaces S, S' , then

$$\bar{\mathbf{r}}(p, q) = \frac{1}{2}\mathbf{r}(p, q) + \frac{1}{2}\mathbf{r}'(p, q)$$

is the parallel parameterisation of \bar{S} . Locally, the definition does not depend on the choice of parallel parameterisations. Needless to say, the normals $\bar{\mathbf{n}}(p, q) = \mathbf{n}(p, q) = \mathbf{n}'(p, q)$ coincide, showing that \bar{S} is also related by parallelism to both S, S' . As a case in point, the middle surface of surfaces \mathbf{r}^\pm defined by formulas (8.2) is \mathbf{r} in the notation from Section 8.

As is well known, every pseudospherical surface carries an asymptotic Chebyshev net [27]. We shall show that for a generic pair of pseudospherical surfaces these nets combine to two concordant nets on the middle surface. This yields the following converse of Theorem 8.2.

Theorem 9.3. Consider two pseudospherical surfaces S, S' of equal constant negative Gaussian curvatures $K = K' = -\kappa^2$. Consider a parallelism between S and S' and the corresponding middle surface \bar{S} . On \bar{S} , consider the images of the asymptotic lines on S, S' under the parallelism. Assuming that no asymptotic direction on S is taken to an asymptotic direction on S' , the images combine to two concordant Chebyshev nets on \bar{S} .

Details are explained in the course of the proof.

Proof. According to Peterson [67, Theorem 4] or Margulies [58, Theorem 4.1], we can find parameters p, q in such a way that

$$\mathbf{r}'_p = \xi \mathbf{r}_p, \quad \mathbf{r}'_q = \eta \mathbf{r}_q. \quad (9.2)$$

To make the exposition self-contained, we give necessary details of the construction of p, q .

In an arbitrary parameterisation, we can write

$$\mathbf{r}'_j = s_j^i \mathbf{r}_i,$$

where s_j^i is called the mapping tensor. In consequence of the Gauss–Weingarten equations (5.2), the compatibility conditions $\mathbf{r}'_{ik} = \mathbf{r}'_{ki}$ take the form of the Margulies equations [58, equation (2.6)], which is

$$s_{i;j}^k = s_{j;i}^k \quad (9.3)$$

(semicolons denote covariant derivatives) and [58, equation (2.7)], which is

$$s_i^k \Pi_{jk} = s_j^k \Pi_{ik}. \quad (9.4)$$

The fundamental forms of S, S' are related by

$$\mathbf{I}'_{ij} = s_i^k s_j^l \mathbf{I}_{kl}, \quad \mathbf{II}'_{ij} = s_i^k \Pi_{kj}, \quad (9.5)$$

their determinants by

$$\det \mathbf{I}' = (\det s)^2 \det \mathbf{I}, \quad \det \mathbf{II}' = \det s \det \mathbf{II}, \quad (9.6)$$

and their Gauss curvatures by

$$K' = K/\det s.$$

By assumption, $K' = K$. Therefore,

$$\det s = 1. \tag{9.7}$$

Now, consider the eigenvalue problem for s in the asymptotic parameterisation of S . Then $\Pi_{11} = \Pi_{22} = 0$, while $\Pi_{12} \neq 0$, whence $s_1^1 = s_2^2$ by equation (9.4). If $s_2^1 s_1^2 = 0$, then either $\Pi'_{11} = 0$ or $\Pi'_{22} = 0$, contrary to the assumptions. Therefore, $s_2^1 s_1^2 \neq 0$ and s has two different eigenvalues $\xi = s_1^1 + \sqrt{s_2^1 s_1^2}$, $\eta = s_1^1 - \sqrt{s_2^1 s_1^2}$ (not to be confused with ξ^\pm , η^\pm of the previous section).

Let X^i be an eigenvector corresponding to the eigenvalue ξ . The vector field $X = X^i \partial_i$ satisfies $X \mathbf{r}' = X^j \mathbf{r}'_{,j} = X^j s_j^i \mathbf{r}_{,i} = \xi X^i \mathbf{r}_{,i} = \xi X \mathbf{r}$ and similarly for Y and η . The two eigenvector directions $[X]$, $[Y]$ are different. Choosing parameters p , q in such a way that $[X] = [\partial_p]$, $[Y] = [\partial_q]$, we obtain equation (9.2). The mapping tensor becomes

$$s = \begin{pmatrix} \xi & 0 \\ 0 & \eta \end{pmatrix}.$$

Formulas (9.5) read

$$\begin{aligned} I'_{11} &= \xi^2 I_{11}, & I'_{12} &= \xi \eta I_{12}, & I'_{22} &= \eta^2 I_{22}, \\ \Pi'_{11} &= \xi \Pi_{11}, & \Pi'_{12} &= \xi \Pi_{12} = \eta \Pi_{12}, & \Pi'_{22} &= \eta \Pi_{22}. \end{aligned}$$

In particular, $\Pi_{12}(\xi - \eta) = 0$. Since $\xi \neq \eta$, we have

$$\Pi'_{12} = \Pi_{12} = 0.$$

Hence, the Peterson coordinates are conjugate on S and S' , which is their well-known property.

Since $\det s = 1$ by equation (9.7), we have

$$\eta = 1/\xi.$$

Denoting $\Delta = \det I$, $\Delta' = \det I'$, equation (9.6) gives

$$\Delta' = \Delta.$$

By assumption, $-\kappa^2 = K = \Pi_{11} \Pi_{22} / \Delta$. Therefore,

$$\Pi_{22} = -\frac{\kappa^2}{\Pi_{11}} \Delta. \tag{9.8}$$

Consider the middle surface $\bar{\mathbf{r}} = \frac{1}{2}(\mathbf{r} + \mathbf{r}')$ now. Using equations (9.2) with $\eta = 1/\xi$, we obtain

$$\mathbf{r}'_p = \frac{1 + \xi}{2} \mathbf{r}_p, \quad \mathbf{r}'_q = \frac{1 + \xi}{2\xi} \mathbf{r}_q.$$

For the first fundamental form, we have

$$\bar{I}_{ij} = \frac{(1 + \xi)^2}{4 \xi^{i+j-2}} I_{ij}, \quad \det \bar{I} = \frac{(1 + \xi)^4}{16 \xi^2} \Delta. \tag{9.9}$$

Note that the metric \bar{I} is singular at $\xi = -1$.

Since $\bar{\mathbf{r}}$, \mathbf{r}' , \mathbf{r} have one and the same normal vector \mathbf{n} , we have $\bar{\Pi}_{ij} = \frac{1}{2}(\Pi_{ij} + \Pi'_{ij})$, that is,

$$\bar{\Pi}_{11} = \frac{1 + \xi}{2} \Pi_{11}, \quad \bar{\Pi}_{12} = 0, \quad \bar{\Pi}_{22} = \frac{1 + \xi}{2\xi} \Pi_{22} = -\frac{1 + \xi}{2\xi} \frac{\kappa^2}{\Pi_{11}} \Delta. \quad (9.10)$$

Thus, the Gaussian curvature of $\bar{\mathbf{r}}$ is

$$\bar{K} = \frac{\det \bar{\Pi}}{\det \bar{\mathbf{I}}} = -\frac{4\kappa^2\xi}{(1 + \xi)^2}. \quad (9.11)$$

We see that the sign of \bar{K} is that of ξ . Moreover, $\xi = -1$ is a true singularity of \bar{S} .

As can be inferred from the results of the previous section, the concordant Chebyshev net on $\bar{\mathbf{r}}$ we look for is expected to follow the asymptotic directions on \mathbf{r} and \mathbf{r}' . Let them be represented by X and X' , respectively. To find the fields X , X' , we look for functions $\zeta(p, q)$, $\zeta'(p, q)$ such that $X = D_p + \zeta D_q$, $X' = D_p + \zeta' D_q$ satisfy $\Pi(X, X) = \Pi'(X', X') = 0$. However,

$$\begin{aligned} \Pi(X, X) &= \Pi_{11} + \zeta^2 \Pi_{22} = \Pi_{11} - \frac{\kappa^2 \zeta^2}{\Pi_{11}} \Delta, \\ \Pi'(X', X') &= \Pi'_{11} + \zeta'^2 \Pi'_{22} = \xi \Pi_{11} - \frac{\kappa^2 \zeta'^2}{\xi \Pi_{11}} \Delta, \end{aligned}$$

whence

$$\zeta = \varepsilon_1 \frac{\Pi_{11}}{\kappa\sqrt{\Delta}}, \quad \zeta' = \varepsilon_2 \frac{\xi \Pi_{11}}{\kappa\sqrt{\Delta}},$$

where $\varepsilon_1, \varepsilon_2$ are ± 1 independently. Altogether we obtain four directions

$$\begin{aligned} X_1 &= D_p + \zeta D_q = D_p + \varepsilon_1 \frac{\Pi_{11}}{\kappa\sqrt{\Delta}} D_q, \\ X_2 &= D_p + \zeta' D_q = D_p + \varepsilon_2 \frac{\xi \Pi_{11}}{\kappa\sqrt{\Delta}} D_q. \end{aligned}$$

In short,

$$X_i = D_p + \varepsilon_i \frac{\xi^{i-1} \Pi_{11}}{\kappa\sqrt{\Delta}} D_q, \quad i = 1, 2.$$

On $\bar{\mathbf{r}}$, the directions $[X_i]$ represent the images of the asymptotic directions on \mathbf{r} , \mathbf{r}' under the parallelism. Hence, they represent the images of the asymptotic lines mentioned in the statement of the theorem.

We shall demonstrate two ways to choose the signs ε_1 and ε_2 so that the net induced on $\bar{\mathbf{r}}$ is concordant Chebyshev. In what follows, geometric objects associated with this net are marked with tilde.

The first fundamental coefficients are

$$\tilde{\bar{I}}_{ij} = \bar{\mathbf{I}}(X_i, X_j) = \bar{I}_{11} + (\varepsilon_i \xi^{i-1} + \varepsilon_j \xi^{j-1}) \frac{\Pi_{11}}{\kappa\sqrt{\Delta}} \bar{I}_{12} + \varepsilon_i \varepsilon_j \xi^{i+j-2} \frac{(\Pi_{11})^2}{\kappa^2 \Delta} \bar{I}_{22},$$

where \bar{I}_{ij} are given by formulas (9.9). Hence,

$$\det \tilde{\bar{\mathbf{I}}} = \frac{(\varepsilon_1 - \varepsilon_2 \xi)^2 (\Pi_{11})^2}{\kappa^2 \Delta} \det \bar{\mathbf{I}} = \frac{(1 + \xi)^4 (\varepsilon_1 - \varepsilon_2 \xi)^2}{16\kappa^2 \xi^2} (\Pi_{11})^2.$$

Likewise, the second fundamental coefficients are

$$\begin{aligned}\tilde{\Pi}_{ij} &= \bar{\Pi}_{11} + (\varepsilon_i \xi^{i-1} + \varepsilon_j \xi^{j-1}) \frac{\Pi_{11}}{\kappa \sqrt{\Delta}} \bar{\Pi}_{12} + \varepsilon_i \varepsilon_j \xi^{i+j-2} \frac{(\Pi_{11})^2}{\kappa^2 \Delta} \bar{\Pi}_{22} \\ &= \frac{1 + \xi}{2} (1 - \varepsilon_i \varepsilon_j \xi^{i+j-3}) \Pi_{11}\end{aligned}$$

by virtue of formulas (9.10). More explicitly,

$$\tilde{\Pi}_{11} = \frac{\xi^2 - 1}{2\xi} \Pi_{11}, \quad \tilde{\Pi}_{12} = \frac{1 + \xi}{2} (1 - \varepsilon_1 \varepsilon_2) \Pi_{11}, \quad \tilde{\Pi}_{22} = \frac{1 - \xi^2}{2} \Pi_{11}.$$

If $\varepsilon_1 = \varepsilon_2$, then $\sigma = \tilde{\Pi}_{12} / \sqrt{\det \tilde{\mathbf{I}}} = 0$, which rules out the concordant net.

Continuing with $\varepsilon_1 \neq \varepsilon_2$, we get

$$\begin{aligned}\det \tilde{\mathbf{I}} &= (1 + \xi)^4 \frac{(\varepsilon_1 - \varepsilon_2 \xi)^2}{16\kappa^2 \xi^2} (\Pi_{11})^2, & \sqrt{\det \tilde{\mathbf{I}}} &= \frac{(1 + \xi)^2}{4} \left| \frac{\varepsilon_1 - \varepsilon_2 \xi}{\xi \kappa} \Pi_{11} \right|, \\ \tilde{\sigma} &= \frac{\tilde{\Pi}_{12}}{\sqrt{\det \tilde{\mathbf{I}}}} = \pm \frac{4\kappa \xi}{(1 + \xi)^2}\end{aligned}$$

according to equation (3.1). The sign \pm depends on whether $\Pi_{11} \geq 0$, $\xi \geq 0$ and $\varepsilon_1 - \varepsilon_2 \xi \geq 0$, being undefined at the singularity $\xi = -1$. Anyway, we have

$$\tilde{K} \pm \kappa \tilde{\sigma} = 0$$

by comparison with equation (9.11) (obviously, $\tilde{K} = \bar{K}$). Consequently, we obtain two concordant nets, one for $\varepsilon_1 = 1$, $\varepsilon_2 = -1$, the other one for $\varepsilon_1 = -1$, $\varepsilon_2 = 1$. Note also that the sign of $\tilde{\sigma}$ is changeable by more than one discrete symmetry, see Table 5.

It remains to be proved that the net has the Chebyshev property, which can be done by proving that $\tilde{\pi}_1 = \tilde{\pi}_2 = 0$ or, equivalently, that $\tilde{\Gamma}_{12}^1 = \tilde{\Gamma}_{21}^2 = 0$. It is a matter of direct verification that the values computed according to equation (3.3) are zero modulo certain valid identities we list in the sequel.

Denoting by $\Gamma_{jk}^i(p, q)$ the Christoffel symbols with respect to the Levi-Civita connection for the metric \mathbf{I} , and by a semicolon the corresponding covariant derivatives, the Mainardi–Codazzi equations $\Pi_{ij;k} - \Pi_{ik;j} = 0$ for \mathbf{r} , cf. equation (5.1), reduce to

$$\begin{aligned}\text{MC}_1 &\equiv \frac{\partial \Pi_{11}}{\partial q} - \Pi_{11} \Gamma_{12}^1 + \Pi_{22} \Gamma_{11}^2 = 0, \\ \text{MC}_2 &\equiv \frac{\partial \Pi_{22}}{\partial p} + \Pi_{11} \Gamma_{22}^1 - \Pi_{22} \Gamma_{12}^2 = 0,\end{aligned}\tag{9.12}$$

where Π_{22} is to be substituted from equation (9.8).

The Margulies equations (9.3) reduce to

$$\begin{aligned}\text{Marg}_1 &\equiv \frac{\partial \xi}{\partial q} - \frac{1 - \xi^2}{\xi} \Gamma_{12}^1 = 0, \\ \text{Marg}_2 &\equiv -\frac{1}{\xi^2} \frac{\partial \xi}{\partial q} + \frac{1 - \xi^2}{\xi} \Gamma_{12}^2 = 0.\end{aligned}\tag{9.13}$$

Now it is straightforward to check that

$$\begin{aligned}\tilde{\Gamma}_{12}^1 &= -\frac{\xi}{1+\xi} \left(\frac{\varepsilon_1}{\sqrt{\Delta}} \text{MC}_1 + \frac{\Pi_{11}}{\kappa\Delta} \text{MC}_2 + \frac{\varepsilon_1^2 - 1}{\varepsilon_1} \frac{\kappa^2 \sqrt{\Delta}}{\Pi_{11}} \Gamma_{11}^2 + (\varepsilon_1^2 - 1) \frac{(\Pi_{11})^2}{\kappa\Delta} \Gamma_{22}^1 \right), \\ \tilde{\Gamma}_{21}^2 &= \frac{\xi}{1+\xi} \left(\frac{\varepsilon_1}{\sqrt{\Delta}} \text{MC}_1 - \kappa \text{Marg}_2 + \frac{\varepsilon_1^2 - 1}{\varepsilon_1} \frac{\kappa^2 \sqrt{\Delta}}{\Pi_{11}} \Gamma_{11}^2 \right) \\ &\quad - \frac{1}{1+\xi} \left(\frac{\Pi_{11}}{\kappa\Delta} \text{MC}_2 + \varepsilon_1 \frac{\Pi_{11}}{\sqrt{\Delta}} \text{Marg}_1 + \frac{\varepsilon_1^2 - 1}{\varepsilon_1} \kappa\Delta (\Pi_{11})^2 \Gamma_{22}^1 \right)\end{aligned}$$

vanish in consequence of equations (9.12) and (9.13) and $\varepsilon_1 = \pm 1$. This finishes the proof of Theorem 9.3. \blacksquare

Theorem 9.3 provides a geometric solution to problem (B). In principle, this geometric solution can be turned into an analytic solution of system (6.5) and (6.6) in implicit form, but the result is too complex to be of any use.

It is worth mentioning that this construction yields Chebyshev nets, but not Chebyshev parameterisations in the sense of Proposition 4.1 (i), which underlines the importance of distinguishing between the two concepts.

Corollary 9.4. *The class of surfaces admitting a concordant Chebyshev net coincides with the class of middle surfaces of pairs of pseudospherical surfaces under the correspondence by equal normals.*

At the end of Section 8, we observed that every concordant net induces a pair of Chebyshev nets on the unit sphere; the explicit description was given in Proposition 8.6. The following proposition provides a version of Theorem 9.3 starting with two Chebyshev nets on the sphere.

Corollary 9.5. *Consider the unit sphere $\|\mathbf{n}\| = 1$ carrying two Chebyshev nets given by directions $[X_1^\pm], [X_2^\pm]$, where (X_1^\pm, X_2^\pm) are two pairs of commuting unit vector fields. Then we can choose the signs in such a way that both X_1^+, X_2^- and X_1^-, X_2^+ represent concordant Chebyshev nets on the surface $\mathbf{r} = \frac{1}{2}\mathbf{r}^+ + \frac{1}{2}\mathbf{r}^-$, where surfaces \mathbf{r}^\pm are determined by the Lelievre formulas*

$$X_1^\pm \mathbf{r}^\pm = -\frac{1}{\kappa} X_1^\pm \mathbf{n} \times \mathbf{n}, \quad X_2^\pm \mathbf{r}^\pm = \frac{1}{\kappa} X_2^\pm \mathbf{n} \times \mathbf{n}$$

and correspond by the parallelism of normals.

Proof. Obvious. Note that $\mathbf{r}^+, \mathbf{r}^-, \mathbf{r}$ correspond to $\mathbf{r}, \mathbf{r}', \bar{\mathbf{r}}$, respectively. \blacksquare

10 Examples

In this section, we discuss explicit examples based on Theorem 9.3. We switch back to the notation of Section 8, cf. Table 1. In particular, $\mathbf{r}^+, \mathbf{r}^-, \mathbf{r}$ of this section are $\mathbf{r}, \mathbf{r}', \bar{\mathbf{r}}$ of Section 9. For the reader's convenience, we review the construction.

Construction 10.1. The input is a pair of pseudospherical surfaces P^+ and P^- .

1. Relate P^+ and P^- by parallelism, i.e., choose parameters p, q so that $\mathbf{n}^+(p, q) = \mathbf{n}^-(p, q)$.
2. Compute the middle surface $\mathbf{r}(p, q) = \frac{1}{2}\mathbf{r}^+(p, q) + \frac{1}{2}\mathbf{r}^-(p, q)$.
3. Find the asymptotic lines on P^+ and P^- , altogether four line families.
4. Find the corresponding four line families on the middle surface.
5. Select the two pairs that form the two concordant Chebyshev nets sought.

Example 10.2. Consider two pseudospheres \mathbf{r}^+ and \mathbf{r}^- with perpendicular axes parallel to the x - and y -axis, respectively. In isodiagonal parameterisations, see Remark 4.3, we have

$$\begin{aligned}\mathbf{r}^+ &= \left[v^+ - \tanh v^+, \frac{\cos u^+}{\cosh v^+}, \frac{\sin u^+}{\cosh v^+} \right], \\ \mathbf{r}^- &= \left[\frac{\cos u^-}{\cosh v^-}, v^- - \tanh v^-, \frac{\sin u^-}{\cosh v^-} \right],\end{aligned}\tag{10.1}$$

assuming $u^\pm \in \mathbb{S}^1$ and $v^\pm \in \mathbb{R}$.

The Gauss maps are almost bijective if using the outward (or inward) normals. Figure 2 is coloured in such a way that the Gauss mapping of the pseudosphere (which is also a parallelism between the pseudosphere and the sphere) is colour-preserving.

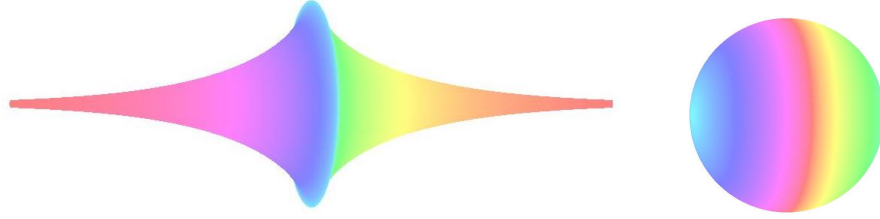


Figure 2. Colour visualisation of the Gauss map by outward normals.

The coordinate formulas are

$$\begin{aligned}\mathbf{n}^+ &= \text{sign } v^+ \left[\frac{1}{\cosh v^+}, \tanh v^+ \cos u^+, \tanh v^+ \sin u^+ \right], \\ \mathbf{n}^- &= \text{sign } v^- \left[\tanh v^- \cos u^-, \frac{1}{\cosh v^-}, \tanh v^- \sin u^- \right],\end{aligned}\tag{10.2}$$

where $\text{sign } v^\pm$ ensure that the normals are outward.

To perform Step 1, we relate parameters u^\pm, v^\pm by $\mathbf{n}^+(u^+, v^+) = \mathbf{n}^-(u^-, v^-)$. This can be done in various ways. Denoting by R_i^\pm and N_i the components of \mathbf{r}^\pm and $\mathbf{n} = \mathbf{n}^\pm$, respectively, the inverse Gauss maps $(\gamma^\pm)^{-1}$ are

$$\begin{aligned}R_1^+ &= \text{sign } N_1 \left(\text{arcosh} \left| \frac{1}{N_1} \right| - \sqrt{1 - N_1^2} \right), & R_i^+ &= \frac{|N_1| N_i}{\sqrt{1 - N_1^2}}, & i &= 2, 3, \\ R_2^- &= \text{sign } N_2 \left(\text{arcosh} \left| \frac{1}{N_2} \right| - \sqrt{1 - N_2^2} \right), & R_i^- &= \frac{N_i |N_2|}{\sqrt{1 - N_2^2}}, & i &= 1, 3,\end{aligned}$$

assuming $N_1^2 + N_2^2 + N_3^2 = 1$. Substituting

$$N_1 = \cos \phi \cos \theta, \quad N_2 = \sin \phi \cos \theta, \quad N_3 = \sin \theta, \quad -\frac{1}{2}\pi < \theta < \frac{1}{2}\pi, \quad -\pi < \phi < \pi,$$

we get $\mathbf{r}^\pm(\phi, \theta)$ in spherical coordinates on the Gauss sphere. Thus,

$$\begin{aligned}\mathbf{r}^+(\phi, \theta) &= \left[\pm \text{arcosh} \left| \frac{1}{\cos \phi \cos \theta} \right| \mp \sqrt{1 - \cos^2 \phi \cos^2 \theta}, \frac{|\cos \phi| \sin \phi \cos^2 \theta}{\sqrt{1 - \cos^2 \phi \cos^2 \theta}}, \right. \\ &\quad \left. \frac{|\cos \phi| \sin \theta \cos \theta}{\sqrt{1 - \cos^2 \phi \cos^2 \theta}} \right], \\ \mathbf{r}^-(\phi, \theta) &= \left[\frac{|\sin \phi| \cos \phi \cos^2 \theta}{\sqrt{1 - \sin^2 \phi \cos^2 \theta}}, \pm \text{arcosh} \left| \frac{1}{\cos \phi \cos \theta} \right| \mp \sqrt{1 - \sin^2 \phi \cos^2 \theta}, \right. \\ &\quad \left. \frac{|\sin \phi| \sin \theta \cos \theta}{\sqrt{1 - \sin^2 \phi \cos^2 \theta}} \right],\end{aligned}$$

where $\pm = \text{sign}(\cos \phi)$.

To perform Step 2, we compute

$$\mathbf{r}(\phi, \theta) = \frac{1}{2}\mathbf{r}^+(\phi, \theta) + \frac{1}{2}\mathbf{r}^-(\phi, \theta). \quad (10.3)$$

This is the middle surface, a snippet of which is displayed in Figure 3 (blue for $0 < \theta < \frac{1}{2}\pi$, yellow for $-\frac{1}{2}\pi < \theta < 0$), $0 < \phi < \frac{1}{2}\pi$, restricted to $x < 2$, $y < 2$. The whole middle surface has four connected components, obtainable by rotating one of them by $\frac{1}{2}\pi$, π , $\frac{3}{2}\pi$ around the z -axis. All parts extend to infinity along the x - and y -axis (here x , y , z refer to coordinates in Euclidean space).

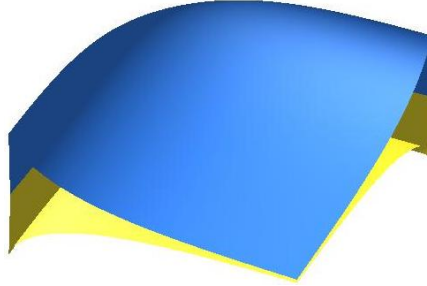


Figure 3. A snippet of the middle surface of two pseudospheres.

The middle surface is regular except eight cuspidal edges, two of which are clearly seen in Figure 3. Their Gauss image consists of four adjacent ovals, formed by zeroes of certain polynomial $\Pi(\cos \phi, \cos \theta)$, which is too large to be printed.⁷ The Gauss images of cuspidal edges are drawn in white in Figure 4 (blue hemisphere for $\theta > 0$, yellow for $\theta < 0$). The Gauss curvature of $R(\phi, \theta)$ is negative for ϕ, θ inside the ovals and positive for ϕ, θ outside the ovals (compare Figures 3 and 4).

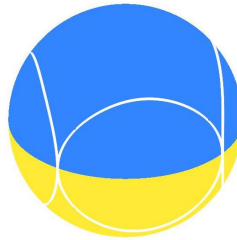


Figure 4. Gaussian images of the cuspidal edges.

Summarising, points (10.3) fill the middle surface and are regular if $\Pi(\cos \phi, \cos \theta) \neq 0$. Figure 5 visualises the middle points for ϕ, θ in different positions relative to the ovals. From left to right, the curvature in $R(\phi, \theta)$ is negative, singular (cuspidal edge) and positive, respectively. The colours indicate individual surfaces (pseudospheres are red and blue, the middle surface is yellow). Short sticks represent outward normals.

In Step 3, we equip the two pseudospheres with their asymptotic Chebyshev parameterisations x^\pm, y^\pm . These can be found by substituting $u^\pm = x^\pm + y^\pm$, $v^\pm = x^\pm - y^\pm$ into (10.1) since u^\pm, v^\pm are isogonal on the pseudospheres \mathbf{r}^\pm . We get

$$\mathbf{r}^+(x^+, y^+) = \left[x^+ - y^+ - \tanh(x^+ - y^+), \frac{\cos(x^+ + y^+)}{\cosh(x^+ - y^+)}, \frac{\sin(x^+ + y^+)}{\cosh(x^+ - y^+)} \right],$$

$$\mathbf{r}^-(x^-, y^-) = \left[\frac{\cos(x^- + y^-)}{\cosh(x^- - y^-)}, x^- - y^- - \tanh(x^- - y^-), \frac{\sin(x^- + y^-)}{\cosh(x^- - y^-)} \right].$$

⁷The ovals $\Pi(\cos \phi, \cos \theta) = 0$ are miraculously well approximated by the ellipses $\phi = \frac{1}{4}\pi(2k - 1 + \cos t)$, $k = 1, \dots, 4$, $\theta = \arccos \sqrt{2 - \sqrt{2}} \cdot \sin t$ in the ϕ, θ -plane.

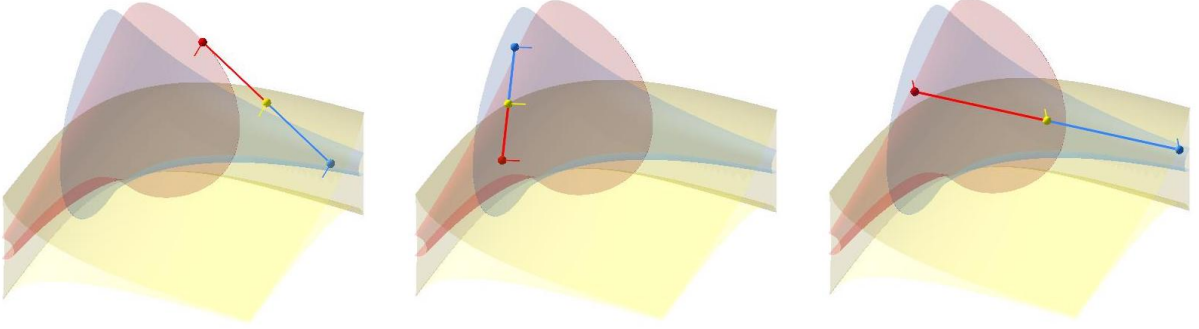


Figure 5. Various positions of $R(\phi, \theta)$.

Figure 6 shows the result.

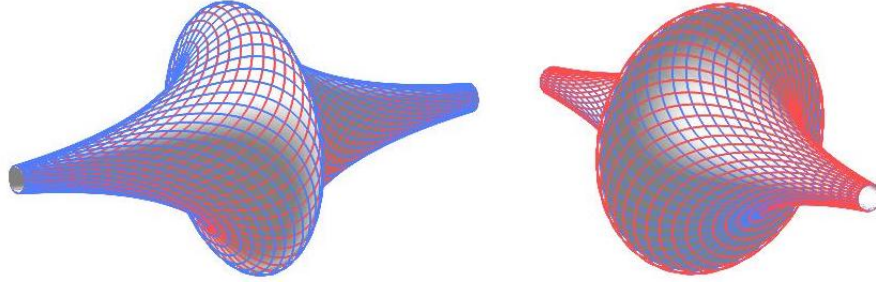


Figure 6. Asymptotic Chebyshev nets on the parent pseudospheres.

In Step 4, we construct the corresponding lines on the middle surface. We first substitute $u^\pm = x^\pm + y^\pm$, $v^\pm = x^\pm - y^\pm$ into (10.2) to get the corresponding Chebyshev nets on the Gaussian spheres, obtaining

$$\mathbf{n}^+ = \left[\frac{1}{\cosh(x^+ - y^+)}, \tanh(x^+ - y^+) \cos(x^+ + y^+), \tanh(x^+ - y^+) \sin(x^+ + y^+) \right],$$

$$\mathbf{n}^- = \left[\tanh(x^- - y^-) \cos(x^- + y^-), \frac{1}{\cosh(x^- - y^-)}, \tanh(x^- - y^-) \sin(x^- + y^-) \right].$$

Denoting by N_1, N_2, N_3 individual components of vectors $\mathbf{n}^+(x^+, y^+)$ and $\mathbf{n}^-(x^-, y^-)$, the map

$$R = \frac{1}{2} \left[\frac{N_1 N_2}{\sqrt{1 - N_2^2}} + \operatorname{arccosh} \left(\frac{1}{N_1} \right) - \sqrt{1 - N_1^2}, \right. \\ \left. \frac{N_1 N_2}{\sqrt{1 - N_1^2}} + \operatorname{arccosh} \left(\frac{1}{N_2} \right) - \sqrt{1 - N_2^2}, \frac{N_1 N_3}{\sqrt{1 - N_1^2}} + \frac{N_2 N_3}{\sqrt{1 - N_2^2}} \right]$$

allows us to obtain explicitly four line families on the middle surface.

In Step 5, we choose appropriate pairs that are guaranteed to form concordant Chebyshev nets by Theorem 9.3. Figure 7 shows the results in the straight and overturned view. Thus, the resulting nets are composed of curves $x^\pm = \text{const}$ and $y^\pm = \text{const}$ corresponding to equally coloured asymptotic curves in Figure 6. They approximate a Chebyshev parameterisation quite well, but actually they only satisfy the curvilinear parallelogram condition, see Section 4. The two nets are different, but identifiable by the mirror symmetry.

Example 10.3. Here we choose \mathbf{r}^+ to be the pseudosphere and \mathbf{r}^- to be one period of a coaxial pseudospherical surface of revolution of elliptic type [8, Section 103]. Positioning the common

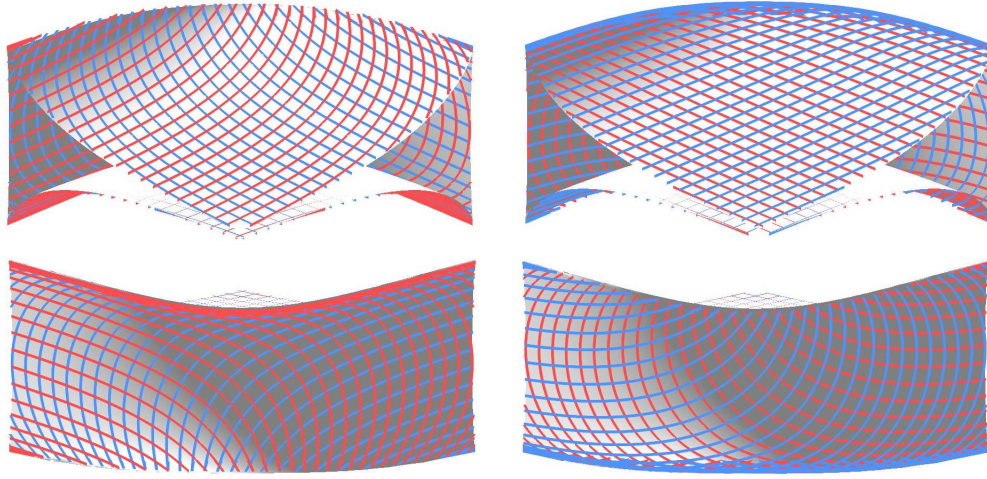


Figure 7. Different concordant Chebyshev nets on the middle surface.

axis in the z -direction, we can write

$$\mathbf{r}^+ = \left[\frac{\cos u^+}{\cosh v^+}, \frac{\sin u^+}{\cosh v^+}, v^+ - \tanh v^+ \right],$$

$$\mathbf{r}^- = \left[\operatorname{sn}(v^- \cos k \mid -\tan^2 k) \cos u^-, \operatorname{sn}(v^- \cos k \mid -\tan^2 k) \sin u^-, \frac{v^- - E(\operatorname{sn}(v^- \cos k \mid -\tan^2 k) \mid -\tan^2 k) \cos k}{\sin k} \right]$$

in the isodiagonal parameterisation. Here sn is the elliptic sine and E is the elliptic integral of the second kind, i.e.,

$$\operatorname{sn}(\phi|m) = \sin \operatorname{am}(\phi|m), \quad E(s|m) = \int_0^s \sqrt{1 - m \sin^2 t} dt.$$

The elliptic amplitude $\operatorname{am}(\phi|m)$ is the inverse of the elliptic integral of the first kind, that is, the value s such that

$$\phi = F(s|m) = \int_0^s \frac{dt}{\sqrt{1 - m \sin^2 t}}.$$

While $u^\pm \in \mathbb{S}^1$, the range of v^\pm will be determined later.

If using the outward normals, the Gauss image of the latter consists of two spherical caps, see Figure 8. In particular, the Gauss map is not surjective.

To perform Step 1, we need formulas for the unit normals (the Gauss maps to \mathbb{S}^2), which are

$$\mathbf{n}^+ = \left[\tanh v^+ \cos u^+, \tanh v^+ \sin u^+, \frac{1}{\cosh v^+} \right],$$

$$\mathbf{n}^- = - \left[\sin k \operatorname{cn}(v^- \cos k \mid -\tan^2 k) \cos u^-, \sin k \operatorname{cn}(v^- \cos k \mid -\tan^2 k) \sin u^-, \cos k \operatorname{dn}(v^- \cos k \mid -\tan^2 k) \right],$$

where $\operatorname{dn}(x|m) = \partial \operatorname{am}(x|m) / \partial x$. The normals point outwards if $v^+ \in [-\operatorname{artanh}(\sin k), 0]$ and $v^- \in [0, K(\sin^2 k)]$, where $K(m) = F(1|m)$ is the complete elliptic integral of the first kind. This choice covers the downward pointing cap of the elliptic pseudospherical surface of revolution and a nozzle-shaped section of the downward pointing half of the pseudosphere if the z -axis is considered vertical, see the two outer surfaces in Figure 9.

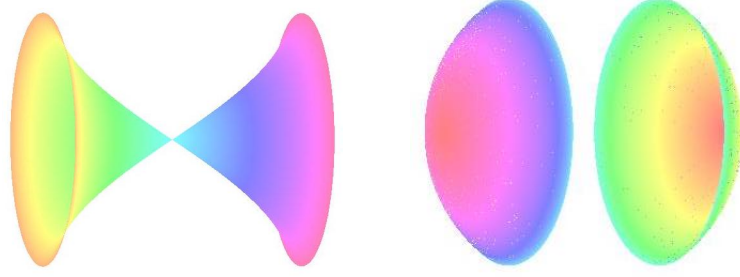


Figure 8. Colour visualisation of the Gauss map in Example 10.3.

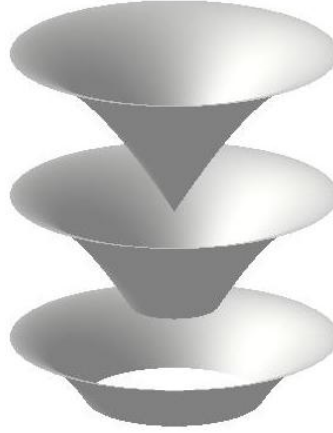


Figure 9. From top to down, the three coaxial surfaces \mathbf{r}^- , \mathbf{r} , \mathbf{r}^+ (separated for visibility).

To obtain the parallelism, we consider the equality $\mathbf{n}^+(u^+, v^+) = \mathbf{n}^-(u^-, v^-)$, which reduces to

$$u^+ = u^-, \quad \sin k \operatorname{cn}(v^- \cos k \mid -\tan^2 k) + \tanh v^+ = 0. \quad (10.4)$$

The latter equation can be solved for v^+ or v^- , giving either

$$u^- = u^+, \quad v^- = \frac{1}{\cos k} \operatorname{arccn} \left(-\frac{\tanh v^+}{\sin k} \mid -\tan^2 k \right),$$

where $v^+ \in [-\operatorname{artanh}(\sin k), 0]$, or

$$u^+ = u^-, \quad v^+ = \operatorname{arcosh} \left(\frac{1}{\operatorname{dn}(v^- \cos k \mid -\tan^2 k) \cos k} \right),$$

where $v^- \in [0, K(\sin^2 k)]$. With the help of these we can switch from the parameterisation by u^+, v^+ to the parameterisation by u^-, v^- and vice versa.

In Step 2, we compute the middle surface. We display only the picture, see Figure 9, suppressing the complicated formulas.

The Gauss curvature of the middle surface is $-2 \sin^2 k / (1 + \sin^2 k)$ at the rim $v^+ = 0$ and tends to zero at the aperture $v^+ = -\operatorname{artanh}(\sin k)$. Thus, although hyperbolic, the middle surface is not pseudospherical.

In Step 3, we have to find the asymptotic Chebyshev parameterisations of the initial surfaces \mathbf{r}^+ , \mathbf{r}^- . As in the previous example, we only have to substitute $u^\pm = x^\pm + y^\pm$, $v^\pm = x^\pm - y^\pm$

into the above formulas for $\mathbf{r}^+(u^+, v^+)$, $\mathbf{r}^-(u^-, v^-)$. The asymptotic Chebyshev net on \mathbf{r}^+ has been visualised above in Figure 6, for \mathbf{r}^- see Figure 10.

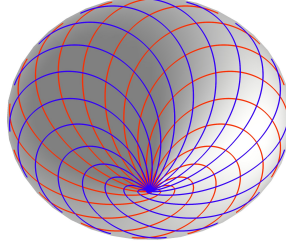


Figure 10. The asymptotic Chebyshev net on \mathbf{r}^- .

To perform Step 4 and find the corresponding nets on the middle surface, we proceed differently from the previous example. In order to be able to write formulas, although only in principle and not fully explicit, we express x^+ , y^- in terms of x^- , y^+ . Eliminating u^\pm , v^\pm from

$$x^\pm + y^\pm = u^+ = u^-, \quad x^\pm - y^\pm = v^\pm$$

and equation (10.4), we get

$$\begin{aligned} x^+ + y^+ &= x^- + y^-, \\ \sin k \operatorname{cn}((x^- - y^-) \cos k \mid -\tan^2 k) + \tanh(x^- + y^+) &= 0. \end{aligned} \quad (10.5)$$

Denoting $w = x^- - y^+$, $v = v^+ = x^+ - y^+$, we substitute

$$x^+ = v + y^+, \quad x^- = w + y^+.$$

into equations (10.5) to get

$$y^- = y^+ + v - w, \quad \sin k \operatorname{cn}((2w - v) \cos k \mid -\tan^2 k) + \tanh v = 0.$$

From the latter equation, we can express w as a function of v , namely

$$w = \Psi_k(v) = \frac{v}{2} + \frac{1}{2 \cos k} \operatorname{arccn} \left(-\frac{\tanh v}{\sin k} \mid -\tan^2 k \right).$$

This opens the way to express v as $\Psi_k^{-1}(w)$ and compute it at least numerically. For the graphs, see Figure 11.

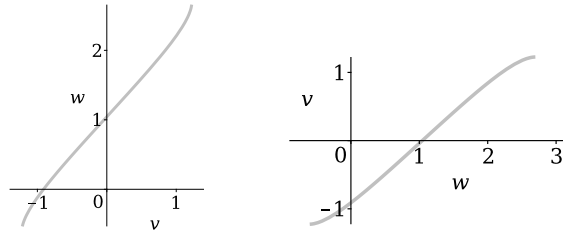


Figure 11. The graphs of $w = \Psi_k(v)$ and $v = \Psi_k^{-1}(w)$ for $k = 1$.

The derivatives are

$$\frac{d\Psi_k(v)}{dv} = \frac{1 + \sqrt{1 - \cos^2 k \cosh^2 v}}{2\sqrt{1 - \cos^2 k \cosh^2 v}}, \quad \frac{d\Psi_k^{-1}(w)}{dw} = \frac{2\sqrt{1 - \cos^2 k \cosh^2 \Psi_k^{-1}(w)}}{1 + \sqrt{1 - \cos^2 k \cosh^2 \Psi_k^{-1}(w)}}.$$

Summarising, the resulting expressions for x^+ , y^- in terms of x^- , y^+ are

$$x^+ = y^+ + \Psi_k^{-1}(x^- - y^+), \quad y^- = 2y^+ - x^- + \Psi_k^{-1}(x^- - y^+).$$

These allow us to obtain parallel parameterisations $\mathbf{r}^+(x^-, y^+)$ and $\mathbf{r}^-(x^-, y^+)$.

By symmetry, we can also write x^- and y^+ in terms of x^+ and y^- and obtain parallel parameterisations $\mathbf{r}^+(x^+, y^-)$ and $\mathbf{r}^-(x^+, y^-)$.

Step 5. The resulting concordant Chebyshev nets are

$$\begin{aligned} \mathbf{r}(x^-, y^+) &= \frac{1}{2}\mathbf{r}^+(x^-, y^+) + \frac{1}{2}\mathbf{r}^-(x^-, y^+), \\ \mathbf{r}(x^+, y^-) &= \frac{1}{2}\mathbf{r}^+(x^+, y^-) + \frac{1}{2}\mathbf{r}^-(x^+, y^-). \end{aligned}$$

For the plots see Figure 12. Again, the two nets are different, but identifiable by the mirror symmetry.

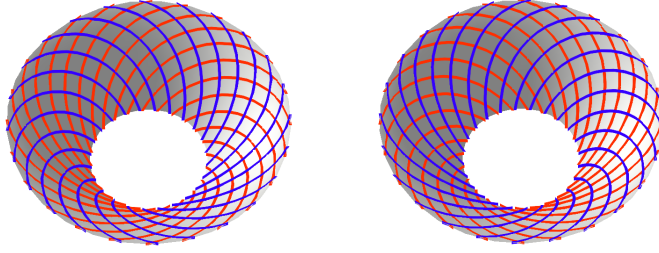


Figure 12. The two concordant Chebyshev nets on the middle surface.

A Appendix on relations among the second-order invariants

As can be inferred from the exposition in Section 2, the geometry of nets in Euclidean space is characterised by the invariance with respect to rigid motions combined with the reparameterisations (2.1).

Consider an isoparametric net $\mathbf{r}(x_1, x_2)$. An r th-order scalar differential invariant, $r \geq 1$, of the net is a scalar expression constructed from the derivatives of \mathbf{r} of order $\leq r$ invariant with respect to rigid motions and transformations (2.1), i.e., with respect to the r -jet prolongation [2] of the vector field

$$F_i(x_i) \frac{\partial}{\partial x_i} + (\mathbf{Q} \cdot \mathbf{r} + \mathbf{P}) \cdot \frac{\partial}{\partial \mathbf{r}},$$

where \mathbf{Q} and \mathbf{P} stand for arbitrary rotation and translation matrices, respectively, while $F_i(x_i)$ are arbitrary functions. Computing routinely the number M_r^{net} of functionally independent scalar differential invariants of order r , we obtain the increments $N_r^{\text{net}} = M_r^{\text{net}} - M_{r-1}^{\text{net}}$ given in Table 2 (so that M_r^{net} is $N_1^{\text{net}} + \dots + N_r^{\text{net}}$). For comparison, we also give the analogous increments N_r^{surf} for invariants of surfaces.

order r	0	1	2	3	4	5	...	r	...
N_r^{net}	0	1	7	10	13	16	...	$3r + 1$...
N_r^{surf}	0	0	2	4	5	6	...	$r + 1$...

Table 2. Growth table of the number of invariants of order r .

As we can see, for surfaces there are just two independent invariants of the second order that can be used to specify a geometric class of surfaces. In contrast, as much as eight independent second-order invariants may be involved in the specification of a geometric class of nets.

The following simple proposition yields another upper bound on the number of independent invariants.

Proposition A.1. *There exist no more than four functionally independent scalar invariants expressible in terms of I_{ij} , Π_{ij} .*

Proof. We have six independent components I_{ij} , Π_{ij} and two independent parameters f_i . ■

Proposition A.2. *In the generic case, the eight independent invariants of order ≤ 2 predicted in Table 2 can be chosen to be the union of any two of $\{\omega, \sigma\}$, $\{K, H\}$, $\{nc_1, nc_2\}$, $\{gt_1, gt_2\}$ along with any two of $\{gc_1, gc_2\}$, $\{\pi_1, \pi_2\}$, $\{\iota_1, \iota_2\}$, $\{\widehat{X}_1\omega, \widehat{X}_2\omega\}$.*

Proof. A straightforward proof goes by computation of Jacobi determinants. ■

The above results imply the existence of mutual relations. A number of them can be found in [74, 75, 76], [83, Chapter 4], [82, Section 93], and later in this section.

Among the known relations we mention the Beetle identities [7, equation (10)]

$$gt_i^2 + nc_i^2 - 2Hnc_i + K = 0$$

and

$$\begin{aligned} gt_1 + gt_2 &= (nc_2 - nc_1) \cot \omega, \\ K &= nc_1nc_2 + gt_1gt_2 + (nc_1gt_2 - nc_2gt_1) \cot \omega, \\ 2H &= nc_1 + nc_2 + (gt_2 - gt_1) \cot \omega, \end{aligned}$$

see [74, 75, 76]. These are polynomial relations homogeneous with respect to the weight equal to the degree in Π_{ij} . Let us look for similar identities incorporating the Schief curvature. Invariants rational in Π_{ij} can be routinely expressed in terms of ω , σ , nc_1 , nc_2 by substituting $\Pi_{ii} = nc_i I_{ii}$ and $\Pi_{12} = \sigma \sqrt{\det I}$, followed by expressing the first-order coefficients in terms of ω . In this way, we easily obtain

$$(-1)^i gt_i = nc_i \cot \omega - \sigma, \tag{A.1}$$

as well as the identities

$$nc_1nc_2 = (K + \sigma^2) \sin^2 \omega, \quad nc_1 + nc_2 = 2(H \sin \omega + \sigma \cos \omega) \sin \omega,$$

from which one can express the curvatures nc_1 and nc_2 in terms of K , H , σ , ω ; then also gt_1 and gt_2 by (A.1). Conversely, if $\cos \omega \neq 0$, then system (A.1) can be solved for σ and $\cot \omega$ as

$$\sigma = \frac{gt_1nc_2 + gt_2nc_1}{nc_2 - nc_1}, \quad \cot \omega = \frac{gt_1 + gt_2}{nc_2 - nc_1}.$$

Finally, the invariants ι_i , π_i , gc_i , $\widehat{X}_i\omega$ expressible in terms of I_{ij} , \widehat{X}_i are related by

$$\pi_i \sin \omega + \widehat{X}_i\omega = (-1)^i gc_i \tag{A.2}$$

and

$$\pi_1 + \pi_2 \cos \omega = \iota_1, \quad \pi_1 \cos \omega + \pi_2 = -\iota_2. \tag{A.3}$$

All these formulas can be proved by straightforward computation.

Let us also mention some simple vector invariants. Recall that $\widehat{X}_1\mathbf{r}$, $\widehat{X}_2\mathbf{r}$ are the unit tangent vectors along the curves of the net. The vectors $\widehat{X}_1\widehat{X}_2\mathbf{r}$, $\widehat{X}_2\widehat{X}_1\mathbf{r}$ are two different invariant versions of what is often referred to as the *twist* in computational geometry ([32, end of Section 7.1] or [6]). It is easily checked that

$$\begin{aligned}\widehat{X}_1\widehat{X}_2\mathbf{r} &= (\sigma \sin \omega)\mathbf{n} + \pi_1\widehat{X}_1\mathbf{r} - (\pi_1 \cos \omega)\widehat{X}_2\mathbf{r}, \\ \widehat{X}_2\widehat{X}_1\mathbf{r} &= (\sigma \sin \omega)\mathbf{n} - \pi_2\widehat{X}_1\mathbf{r} + (\pi_2 \cos \omega)\widehat{X}_2\mathbf{r}.\end{aligned}\tag{A.4}$$

Then

$$[\widehat{X}_1, \widehat{X}_2]\mathbf{r} = \widehat{X}_1\widehat{X}_2\mathbf{r} - \widehat{X}_2\widehat{X}_1\mathbf{r} = (\pi_1 + \pi_2 \cos \omega)\widehat{X}_1\mathbf{r} - (\pi_1 \cos \omega + \pi_2)\widehat{X}_2\mathbf{r}$$

proves formula (A.3). Furthermore, $\widehat{X}_1\mathbf{n}$, $\widehat{X}_2\mathbf{n}$ are tangent vectors to the surface that reflect the change of the normal vector to the surface along the curves of the net. In matrix notation, we have

$$\begin{pmatrix} \widehat{X}_1\mathbf{r} \\ \widehat{X}_2\mathbf{r} \end{pmatrix} \begin{pmatrix} \widehat{X}_1\mathbf{n} & \widehat{X}_2\mathbf{n} \end{pmatrix} = - \begin{pmatrix} \widehat{X}_1\widehat{X}_1\mathbf{r} & \widehat{X}_1\widehat{X}_2\mathbf{r} \\ \widehat{X}_2\widehat{X}_1\mathbf{r} & \widehat{X}_2\widehat{X}_2\mathbf{r} \end{pmatrix} \cdot \mathbf{n} = - \begin{pmatrix} \text{nc}_1 & \sigma \\ \sigma & \text{nc}_2 \end{pmatrix} \sin \omega,$$

which demonstrates a kinship between σ and the normal curvatures.

Finally, $\widehat{X}_1\mathbf{n} \cdot \widehat{X}_2\mathbf{n}$ equals $K \sin \omega \cot \omega_{\text{III}}$, where ω_{III} is the intersection angle of the spherical image of the net. Moreover,

$$\cot \omega_{\text{III}} = \frac{2H\sigma}{K} - \cot \omega.\tag{A.5}$$

To conclude this section, we review five discrete symmetries of nets described in Tables 3 and 4. Their action on the invariants is summarised in Table 5.

T_{-1}	Reversion of the protractor, $\omega \longleftrightarrow -\omega$
T_0	Change of sign of all vector and triple products (the orientation of Euclidean space)
T_1	Change of orientation of curves of the first family
T_2	Change of orientation of curves of the second family
T_3	Family swap

Table 3. Five discrete symmetries of nets in Euclidean space.

	X_1	X_2	\mathbf{n}	I_{11}	I_{12}	I_{22}	II_{11}	II_{12}	II_{22}
T_{-1}	X_1	X_2	\mathbf{n}	I_{11}	$-I_{12}$	I_{22}	II_{11}	II_{12}	II_{22}
T_0	X_1	X_2	$-\mathbf{n}$	I_{11}	I_{12}	I_{22}	$-\text{II}_{11}$	$-\text{II}_{12}$	$-\text{II}_{22}$
T_1	$-X_1$	X_2	\mathbf{n}	I_{11}	$-I_{12}$	I_{22}	II_{11}	$-\text{II}_{12}$	II_{22}
T_2	X_1	$-X_2$	\mathbf{n}	I_{11}	$-I_{12}$	I_{22}	II_{11}	$-\text{II}_{12}$	II_{22}
T_3	X_2	X_1	\mathbf{n}	I_{22}	I_{12}	I_{11}	II_{22}	II_{12}	II_{11}

Table 4. The action of discrete symmetries on X_i , \mathbf{n} , I_{ij} and II_{ij} .

The action on ω_{III} is the same as on ω . Needless to say, all the identities among invariants we have listed in this section are invariant under transformations T_{-1}, \dots, T_3 .

	ω	H	σ	nc_2	nc_1	gc_1	gc_2	gt_1	gt_2	π_1	π_2	ι_1	ι_2	$\omega_{,1}$	$\omega_{,2}$
T_{-1}	$-\omega$	H	$-\sigma$	nc_1	nc_2	$-gc_1$	$-gc_2$	$-gt_1$	$-gt_2$	π_1	π_2	ι_1	ι_2	$-\omega_{,1}$	$\omega_{,2}$
T_0	ω	$-H$	$-\sigma$	$-nc_1$	$-nc_2$	gc_1	gc_2	$-gt_1$	$-gt_2$	π_1	π_2	ι_1	ι_2	$\omega_{,1}$	$\omega_{,2}$
T_1	$\pi - \omega$	H	$-\sigma$	nc_1	nc_2	gc_1	$-gc_2$	$-gt_1$	$-gt_2$	π_1	$-\pi_2$	ι_1	$-\iota_2$	$\omega_{,1}$	$-\omega_{,2}$
T_2	$\pi - \omega$	H	$-\sigma$	nc_1	nc_2	$-gc_1$	gc_2	$-gt_1$	$-gt_2$	$-\pi_1$	π_2	$-\iota_1$	ι_2	$-\omega_{,1}$	$\omega_{,2}$
T_3	ω	H	σ	nc_2	nc_1	$-gc_2$	$-gc_1$	$-gt_2$	$-gt_1$	π_2	π_1	$-\iota_2$	$-\iota_1$	$\omega_{,2}$	$\omega_{,1}$

Table 5. The action of discrete symmetries on the invariants.

Conclusions and perspectives

After reviewing nets and their second-order invariants, we introduced integrable classes of nets in analogy with integrable classes of surfaces. Then, starting from an earlier result [48], we established equivalence of concordant Chebyshev nets and pairs of pseudospherical surfaces. The integrability of concordant Chebyshev nets, which we first observed in [48], is hereby explicitly related to the integrability of pseudospherical surfaces. Presented examples are the concordant Chebyshev nets on the middle surface of two pseudospheres and on the middle surface of the pseudosphere and another coaxial axisymmetric pseudospherical surface.

In the outlook, we identify the following tasks:

- Explore the full “parameter space” in Figure 1.
- Explore the other integrable Chebyshev nets from paper [48].
- Employ the ZCRs found in paper [48] to obtain recursion operators, solutions, etc.
- Use the methods of papers [5, 48] to search for new integrable classes of nets.
- Explore higher-dimensional analogues.

Acknowledgements

This research received support from MŠMT under RVO 47813059. The author is grateful to Evgeny Ferapontov and Jan Cieřliński for introduction into integrable surfaces and thought-provoking discussions that inspired this particular research.

References

- [1] Agafonov S.I., Quadratic integrals of geodesic flow, webs, and integrable billiards, *J. Geom. Phys.* **161** (2021), 104041, 7 pages, [arXiv:2004.12374](#).
- [2] Alekseevskij D.V., Vinogradov A.M., Lychagin V.V., Basic ideas and concepts of differential geometry, in Geometry I, Editor R.V. Gamkrelidze, *Encyclopaedia Math. Sci.*, Vol. 28, Springer, Berlin, 1991, 1–264.
- [3] Aoust A., Analyse infinitésimale des courbes tracées sur une surface quelconque, Gauthier-Villars, Paris, 1869.
- [4] Baran H., Marvan M., On integrability of Weingarten surfaces: a forgotten class, *J. Phys. A* **42** (2009), 404007, 16 pages, [arXiv:1002.0989](#).
- [5] Baran H., Marvan M., Classification of integrable Weingarten surfaces possessing an $\mathfrak{sl}(2)$ -valued zero curvature representation, *Nonlinearity* **23** (2010), 2577–2597, [arXiv:1002.0992](#).
- [6] Barnhill R.E., Farin G., Fayard L., Hagen H., Twists, curvatures and surface interrogation, *Comput. Aided Des.* **20** (1988), 341–344, 345–346.
- [7] Beetle R.D., A formula in the theory of surfaces, *Ann. of Math.* **15** (1913–1914), 179–183.
- [8] Bianchi L., *Lezioni di Geometria Differenziale*, Vol. 1, E. Spoerri, Pisa, 1902.
- [9] Bianchi L., *Lezioni di Geometria Differenziale*, Vol. 2, E. Spoerri, Pisa, 1903.

- [10] Bianchi L., Le reti di Tchebychef sulle superficie ed il parallelismo nel senso di Levi-Civita, *Boll. Unione Mat. Ital.* **1** (1922), 1–6.
- [11] Bobenko A.I., Surfaces in terms of 2 by 2 matrices. Old and new integrable cases, in Harmonic Maps and Integrable Systems, Editors A.P. Fordy, J.C. Wood, *Aspects Math.*, Vol. E23, Friedr. Vieweg, Braunschweig, 1994, 83–127.
- [12] Bobenko A.I., Pinkall U., Discretization of surfaces and integrable systems, in Discrete Integrable Geometry and Physics (Vienna, 1996), Editors A.I. Bobenko, R. Seiler, *Oxford Lecture Ser. Math. Appl.*, Vol. 16, Oxford University Press, New York, 1999, 3–58.
- [13] Bobenko A.I., Pottmann H., Rörig T., Multi-nets. Classification of discrete and smooth surfaces with characteristic properties on arbitrary parameter rectangles, *Discrete Comput. Geom.* **63** (2020), 624–655, [arXiv:1802.05063](https://arxiv.org/abs/1802.05063).
- [14] Bobenko A.I., Suris Yu.B., Discrete differential geometry. Integrable structure, *Grad. Stud. Math.*, Vol. 98, American Mathematical Society, Providence, RI, 2008.
- [15] Bortolotti E., Su alcune questioni di geometria delle superficie, *Boll. Unione Mat. Ital.* **4** (1925), 162–166.
- [16] Brander D., Pseudospherical surfaces with singularities, *Ann. Mat. Pura Appl.* **196** (2017), 905–928, [arXiv:1502.04876](https://arxiv.org/abs/1502.04876).
- [17] Bruce J.W., Tari F., On binary differential equations, *Nonlinearity* **8** (1995), 255–271.
- [18] Catalano Ferraioli D., de Oliveira Silva L.A., Nontrivial 1-parameter families of zero-curvature representations obtained via symmetry actions, *J. Geom. Phys.* **94** (2015), 185–198.
- [19] Chebyshev P.L., On the cutting of garments, *Russian Math. Surveys* **1** (1946), no. 2, 38–42.
- [20] Chern S.-S., Tenenblat K., Foliations on a surface of constant curvature and the modified Korteweg–de Vries equations, *J. Differential Geometry* **16** (1981), 347–349.
- [21] Cieśliński J., Nonlocal symmetries and a working algorithm to isolate integrable geometries, *J. Phys. A* **26** (1993), L267–L271.
- [22] Cieśliński J., Goldstein P., Sym A., Isothermic surfaces in \mathbf{E}^3 as soliton surfaces, *Phys. Lett. A* **205** (1995), 37–43, [arXiv:solv-int/9502004](https://arxiv.org/abs/solv-int/9502004).
- [23] Darboux G., Leçons sur la théorie générale des surfaces, Première Partie, Gauthier-Villars, Paris, 1887.
- [24] Darboux G., Leçons sur la théorie générale des surfaces, Deuxième Partie, Gauthier-Villars, Paris, 1889.
- [25] Darboux G., Leçons sur la théorie générale des surfaces, Troisième Partie, Gauthier-Villars, Paris, 1894.
- [26] Décaillot A.-M., Géométrie des tissus. Mosaiques. Échiquiers. Mathématiques curieuses et utiles, *Rev. Histoire Math.* **8** (2002), 145–206.
- [27] Dini U., Sopra alcune formole generali della teoria delle superficie, e loro applicazioni, *Ann. Mat. Pura Appl.* **4** (1870), 175–206.
- [28] Dubnov Ya.S., Semitensors of a two-dimensional net, *Izv. Vyssh. Uchebn. Zaved. Mat.* (1958), no. 3, 74–83.
- [29] Dubrovin B.A., Theta-functions and nonlinear equations, *Russian Math. Surveys* **36** (1981), no. 2, 11–92.
- [30] Eisenhart L.P., Three particular systems of lines on a surface, *Trans. Amer. Math. Soc.* **5** (1904), 421–437.
- [31] Eisenhart L.P., A treatise on the differential geometry of curves and surfaces, Ginn, Boston, 1909.
- [32] Faux I.D., Pratt M.J., Computational geometry for design and manufacture, Math. Appl., Ellis Horwood, Chichester, 1979.
- [33] Fuchs D., Tabachnikov S., Mathematical omnibus. Thirty lectures on classic mathematics, American Mathematical Society, Providence, RI, 2007.
- [34] Gambier B., Surfaces de Voss-Guichard, *Ann. Sci. École Norm. Sup.* **48** (1931), 359–396.
- [35] Ghys É., Sur la coupe des vêtements: variation autour d’un thème de Tchebychev, *Enseign. Math.* **57** (2011), 165–208.
- [36] Graustein W.C., Parallel maps of surfaces, *Trans. Amer. Math. Soc.* **23** (1922), 298–332.
- [37] Graustein W.C., Parallelism and equidistance in classical differential geometry, *Trans. Amer. Math. Soc.* **34** (1932), 557–593.
- [38] Green G.M., Nets of space curves, *Trans. Amer. Math. Soc.* **21** (1920), 207–236.

- [39] Gürses M., Tek S., Integrable curves and surfaces, in Proceedings of the 17th International Conference “Geometry, Integrability and Quantization” (Sts. Constantine and Elena, June 5–10, 2015), Editors I.M. Mladenov, G. Meng, A. Yoshioka, *Geom. Integrability Quantization*, Vol. 17, [Bulgarian Academy of Sciences](#), Sofia, 2016, 13–71.
- [40] Hasimoto H., A soliton on a vortex filament, *J. Fluid Mech.* **51** (1972), 477–485.
- [41] Howell P.D., Ockendon H., Ockendon J.R., Draping woven sheets, *ANZIAM J.* **62** (2020), 355–385.
- [42] Kagan V.F., Fundamentals of the theory of surfaces in tensorial representation II, Gostechizdat, Moskva, 1948.
- [43] Khesin B., Tabachnikov S., Polar bear or penguin? Musings on earth cartography and Chebyshev nets, *Math. Intelligencer* **43** (2021), 20–24.
- [44] Kilian M., Müller C., Tervooren J., Smooth and discrete cone-nets, *Results Math.* **78** (2023), 110, 40 pages.
- [45] Koch R., Parallelogrammnetze, *Monatsh. Math.* **86** (1979), 265–284.
- [46] Koch R., Diagonale Tschebyscheff-Netze, *Abh. Math. Sem. Univ. Hamburg* **52** (1982), 43–66.
- [47] Konopel’chenko B.G., Nets in \mathbb{R}^3 , their integrable evolutions and the DS hierarchy, *Phys. Lett. A* **183** (1993), 153–159.
- [48] Krasil’shchik J., Marvan M., Coverings and integrability of the Gauss–Mainardi–Codazzi equations, *Acta Appl. Math.* **56** (1999), 217–230, [arXiv:solv-int/9812010](#).
- [49] Kuznetsov E.N., Underconstrained structural systems, Mech. Engrg. Ser., [Springer](#), New York, 1991.
- [50] Lamb Jr. G.L., Solitons on moving space curves, *J. Math. Phys.* **18** (1977), 1654–1661.
- [51] Levi D., Sym A., Tu G.-Z., A working algorithm to isolate integrable surfaces in E^3 , Preprint DF INFN Roma 761, 1990.
- [52] Liddell I., Frei Otto and the development of gridshells, *Case Stud. Struct. Eng.* **4** (2015), 39–49.
- [53] Lie S., Beiträge zur Theorie der Minimalflächen. I. Projectivische Untersuchungen über algebraische Minimalflächen, *Math. Ann.* **14** (1878), 331–416.
- [54] von Lilienthal R., Die auf einer Fläche gezogenen Kurven, in Enzyklopädie der Mathematischen Wissenschaften mit Einschluß ihrer Anwendungen, Teubner, Leipzig, 1902, 105–183.
- [55] Lin R., Conte R., On a surface isolated by Gambier, *J. Nonlinear Math. Phys.* **25** (2018), 509–514, [arXiv:1805.10450](#).
- [56] Liu D., Pellis D., Chiang Y.-C., Rist F., Wallner J., Pottmann H., Deployable strip structures, *ACM Trans. Graph.* **42** (2023), 103, 16 pages.
- [57] Mack C., Taylor H.M., The fitting of woven cloth to surfaces, *J. Text. Inst. Trans.* **47** (1956), T477–T488.
- [58] Margulies G., Peterson’s theorem on surfaces corresponding by parallelism. I, *Proc. Amer. Math. Soc.* **12** (1961), 577–587.
- [59] Marvan M., Reducibility of zero curvature representations with application to recursion operators, *Acta Appl. Math.* **83** (2004), 39–68, [arXiv:nlin.SI/0306006](#).
- [60] Marvan M., On the spectral parameter problem, *Acta Appl. Math.* **109** (2010), 239–255, [arXiv:0804.2031](#).
- [61] Masson Y., Existence and construction of Chebyshev nets with singularities and application to gridshells, Ph.D. thesis, Université Paris Est, 2017, available at <https://theses.hal.science/tel-01676984v1>.
- [62] Masson Y., Monasse L., Existence of global Chebyshev nets on surfaces of absolute Gaussian curvature less than 2π , *J. Geom.* **108** (2017), 25–32.
- [63] Matveev V.B., 30 years of finite-gap integration theory, *Philos. Trans. R. Soc. Lond. Ser. A Math. Phys. Eng. Sci.* **366** (2008), 837–875.
- [64] Montagne N., Douthe C., Tellier X., Fivet C., Baverel O., Voss surfaces: A design space for geodesic gridshells, in Inspiring the Next Generation (Proc. IASS Annual Symp. 2020 and 7th Int. Conf. Spatial Structures), Editors S.A. Behnejad, G.A.R. Parke and O.A. Samavati, [Spatial Structures Research Centre University Surrey](#), UK, 2021, 3473–3483.
- [65] Mukherjee R., Balakrishnan R., Moving curves of the sine-Gordon equation: new links, *Phys. Lett. A* **372** (2008), 6347–6362.
- [66] Norden A.P., Theory of surfaces, GITTL, Moscow, 1956.
- [67] Peterson K.M., Sur les relations et les affinités entre les surfaces courbes, *Ann. Fac. Sci. Univ. Toulouse* **7** (1905), 5–43, translated from Russian: *Mat. Sb.* **1** (1866), 391–438.

- [68] Pottmann H., Eigensatz M., Vaxman A., Wallner J., Architectural geometry, *Comput. Graph.* **47** (2015), 145–164.
- [69] Rogers C., Schief W.K., Bäcklund and Darboux transformations. Geometry and modern applications in soliton theory, *Cambridge Texts Appl. Math.*, Cambridge University Press, Cambridge, 2002.
- [70] Sageman-Furnas A.O., Chern A., Ben-Chen M., Vaxman A., Chebyshev nets from commuting PolyVector fields, *ACM Trans. Graph.* **38** (2019), 172, 16 pages.
- [71] Sannia G., Geometria differenziale dei reticolati piani invariante per un gruppo di collineazioni, *Rend. Circ. Mat. Palermo* **48** (1924), 289–307.
- [72] Sauer R., Weckelige Kurvenetze bei einer infinitesimalen Flächenverbiegung, *Math. Ann.* **108** (1933), 673–693.
- [73] Sauer R., Differenzengeometrie, Springer, Berlin, 1970.
- [74] Scherrer W., Die Grundgleichungen der Flächentheorie. I, *Comment. Math. Helv.* **29** (1955), 180–198.
- [75] Scherrer W., Die Grundgleichungen der Flächentheorie. II, *Comment. Math. Helv.* **32** (1957), 73–84.
- [76] Scherrer W., Die Grundgleichungen der Flächentheorie. III, *Comment. Math. Helv.* **37** (1962), 177–197.
- [77] Schief W.K., On the integrability of Bertrand curves and Razzaboni surfaces, *J. Geom. Phys.* **45** (2003), 130–150.
- [78] Schief W.K., Discrete Chebyshev nets and a universal permutability theorem, *J. Phys. A* **40** (2007), 4775–4801.
- [79] Schief W.K., Rogers C., Binormal motion of curves of constant curvature and torsion. Generation of soliton surfaces, *R. Soc. Lond. Proc. Ser. A Math. Phys. Eng. Sci.* **455** (1999), 3163–3188.
- [80] Servant M., Sur l’habillage des surfaces, *C. R. Acad. Sci.* **137** (1903), 112–115.
- [81] Shin H.J., Lund–Regge vortex strings in terms of Weierstrass elliptic functions, *Nuclear Phys. B* **624** (2002), 431–451.
- [82] Shulikovskiy V.I., Classical differential geometry, GIFML, Moscow, 1963.
- [83] Spivak M., A comprehensive introduction to differential geometry. Vol. III, Publish or Perish, Inc., Boston, MA, 1975.
- [84] Sym A., Soliton surfaces and their applications (soliton geometry from spectral problems), in Geometric Aspects of the Einstein Equations and Integrable Systems (Scheveningen, 1984), *Lecture Notes in Phys.*, Vol. 239, Springer, Berlin, 1985, 154–231.
- [85] Tellier X., Bundling elastic gridshells with alignable nets. Part I: Analytical approach, *Autom. Constr.* **141** (2022), 104291, 36 pages.
- [86] Tian C., Foliation on a surface of constant curvature and some nonlinear evolution equations, *Chinese Ann. Math. Ser. B* **9** (1988), 118–122.
- [87] Toda M., On a duality property of isothermic surfaces, *JP J. Geom. Topol.* **20** (2017), 85–90.
- [88] Vashpanova T.Yu., Bezkorovaynaya L.L., LGT-network of a surface and its properties, *Visn. Kyiv. Univ. im. Tarasa Shevchenka, Ser. Fiz.-Mat. Nauk* **2010** (2010), no. 2, 7–11.
- [89] Vaxman A., Campen M., Diamanti O., Panozzo D., Bommès D., Hildebrandt K., Ben-Chen M., Directional field synthesis, design, and processing, *Comput. Graph. Forum* **35** (2016), 545–572.
- [90] Voss A., Ueber ein neues Princip der Abbildung krummer Oberflächen, *Math. Ann.* **19** (1881), 1–26.
- [91] Wang H., Pottmann H., Characteristic parameterizations of surfaces with a constant ratio of principal curvatures, *Comput. Aided Geom. Design* **93** (2022), 102074, 23 pages.
- [92] Weatherburn C.E., On Levi-Civita’s theory of parallelism, *Bull. Amer. Math. Soc.* **34** (1928), 585–590.
- [93] Weise K.H., Invariante Charakterisierung von Kurvennetzen, *Math. Z.* **46** (1940), 665–691.
- [94] Whittmore J.K., Total geodesic curvature and geodesic torsion, *Bull. Amer. Math. Soc.* **29** (1923), 51–54.
- [95] Wolf T., A comparison of four approaches to the calculation of conservation laws, *European J. Appl. Math.* **13** (2002), 129–152.
- [96] Zakharov V.E., Shabat A.B., Integration of nonlinear equations of mathematical physics by the method of inverse scattering. II, *Funct. Anal. Appl.* **13** (1979), 166–174.